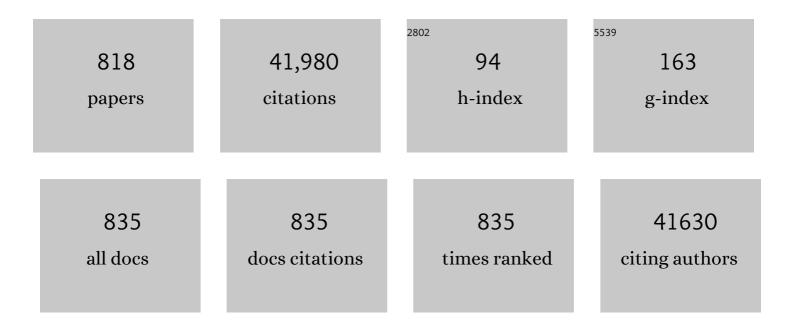
List of Publications by Year in descending order

Source: https://exaly.com/author-pdf/1274187/publications.pdf Version: 2024-02-01



IVAN D DADKIN

#	Article	IF	CITATIONS
1	Mo/Fe bimetallic pyrophosphates derived from Prussian blue analogues for rapid electrocatalytic oxygen evolution. Green Energy and Environment, 2023, 8, 1450-1458.	8.7	4
2	Progress and Perspectives of Organosulfur for Lithium–Sulfur Batteries. Advanced Energy Materials, 2022, 12, 2103483.	19.5	69
3	Liquid-microjet photoelectron spectroscopy of the green fluorescent protein chromophore. Nature Communications, 2022, 13, 507.	12.8	10
4	A route to engineered high aspect-ratio silicon nanostructures through regenerative secondary mask lithography. Nanoscale, 2022, 14, 1847-1854.	5.6	7
5	Electron-Deficient Au Nanoparticles Confined in Organic Molecular Cages for Catalytic Reduction of 4-Nitrophenol. ACS Applied Nano Materials, 2022, 5, 1276-1283.	5.0	21
6	Universal Theory of Light Scattering of Randomly Oriented Particles: A Fluctuational-Electrodynamics Approach for Light Transport Modeling in Disordered Nanostructures. ACS Photonics, 2022, 9, 672-681.	6.6	2
7	Identification and manipulation of dynamic active site deficiency-induced competing reactions in electrocatalytic oxidation processes. Energy and Environmental Science, 2022, 15, 2386-2396.	30.8	71
8	A light–heat synergism in the sub-bandgap photocatalytic response of pristine TiO <sub>2</sub> : a study of <i>in situ</i> diffusion reflectance and conductance. Physical Chemistry Chemical Physics, 2022, 24, 5618-5626.	2.8	4
9	Facile formation of black titania films using an atmospheric-pressure plasma jet. Green Chemistry, 2022, 24, 2499-2505.	9.0	3
10	Strong robust superhydrophobic C/silicone monolith for photothermal ice removal. Journal of Materials Science, 2022, 57, 6963-6970.	3.7	8
11	A Universal Polyiodide Regulation Using Quaternization Engineering toward High Valueâ€Added and Ultraâ€Stable Zincâ€Iodine Batteries. Advanced Science, 2022, 9, e2105598.	11.2	58
12	Adsorptivity of Some Organic Compounds to Copper Nanoparticles. International Journal of Self-Propagating High-Temperature Synthesis, 2022, 31, 47-50.	0.5	0
13	Hydrogenation of Xylenes, Ethylbenzene, and Isopropylbenzene on Ni Nanoparticles. International Journal of Self-Propagating High-Temperature Synthesis, 2022, 31, 42-46.	0.5	0
14	Ultra-stretchable and superhydrophobic textile-based bioelectrodes for robust self-cleaning and personal health monitoring. Nano Energy, 2022, 97, 107160.	16.0	64
15	Fabrication of C-Doped Titanium Dioxide Coatings with Improved Anti-icing and Tribological Behavior. Langmuir, 2022, 38, 576-583.	3.5	5
16	Topochemistryâ€Driven Synthesis of Transitionâ€Metal Selenides with Weakened Van Der Waals Force to Enable 3Dâ€Printed Naâ€Ion Hybrid Capacitors. Advanced Functional Materials, 2022, 32, .	14.9	91
17	Rationally Designed Sodium Chromium Vanadium Phosphate Cathodes with Multiâ€Electron Reaction for Fastâ€Charging Sodiumâ€lon Batteries. Advanced Energy Materials, 2022, 12, .	19.5	71
18	Mussel-Inspired Interfacial Modification for Ultra-Stable MoS <sub>2</sub> Lubricating Films with Improved Tribological Behavior on Nano-Textured ZnO Surfaces Using the AACVD Method. ACS Applied Materials & Interfaces, 2022, 14, 27484-27494.	8.0	7

#	Article	IF	CITATIONS
19	Robust superamphiphobic coatings with gradient and hierarchical architecture and excellent anti-flashover performances. Nano Research, 2022, 15, 7565-7576.	10.4	10
20	Durable fire retardant, superhydrophobic, abrasive resistant and air/UV stable coatings. Journal of Colloid and Interface Science, 2021, 582, 301-311.	9.4	39
21	Some peculiarities of room-temperature ferromagnetism in ensembles of mixed-phase TiNx-TiOy nanoparticles. Materials Research Bulletin, 2021, 134, 111092.	5.2	5
22	Supersaturated bridge-sulfur and vanadium co-doped MOS2 nanosheet arrays with enhanced sodium storage capability. Nano Research, 2021, 14, 74-80.	10.4	42
23	Assessment of GaPSb/Si tandem material association properties for photoelectrochemical cells. Solar Energy Materials and Solar Cells, 2021, 221, 110888.	6.2	4
24	Sol–Gel Synthesis of Highâ€Density Zeolitic Imidazolate Framework Monoliths via Ligand Assisted Methods: Exceptional Porosity, Hydrophobicity, and Applications in Vapor Adsorption. Advanced Functional Materials, 2021, 31, 2008357.	14.9	32
25	Ambient Fabrication of Organic–Inorganic Hybrid Perovskite Solar Cells. Small Methods, 2021, 5, e2000744.	8.6	63
26	Unprecedented enhancement of wear resistance for epoxy-resin graphene composites. Nanoscale, 2021, 13, 2855-2867.	5.6	34
27	Copper as an antimicrobial agent: recent advances. RSC Advances, 2021, 11, 18179-18186.	3.6	118
28	The bionic sunflower: a bio-inspired autonomous light tracking photocatalytic system. Energy and Environmental Science, 2021, 14, 3931-3937.	30.8	39
29	Alleviation of Dendrite Formation on Zinc Anodes via Electrolyte Additives. ACS Energy Letters, 2021, 6, 395-403.	17.4	340
30	Palladium alloys used as electrocatalysts for the oxygen reduction reaction. Energy and Environmental Science, 2021, 14, 2639-2669.	30.8	158
31	The effect of Cu dopants on electron transfer to O <sub>2</sub> and the connection with acetone photocatalytic oxidations over nano-TiO <sub>2</sub> . Physical Chemistry Chemical Physics, 2021, 23, 8300-8308.	2.8	6
32	Nonfluoride-modified halloysite nanotube-based hybrid: potential for acquiring super-hydrophobicity and improving flame retardancy of epoxy resin. Journal of Nanostructure in Chemistry, 2021, 11, 353-366.	9.1	9
33	Bandwidth limits of luminescent solar concentrators as detectors in free-space optical communication systems. Light: Science and Applications, 2021, 10, 3.	16.6	45
34	Charge Transport Phenomena in Heterojunction Photocatalysts: The WO <sub>3</sub> /TiO <sub>2</sub> System as an Archetypical Model. ACS Applied Materials & Interfaces, 2021, 13, 9781-9793.	8.0	24
35	Zn and N Codoped TiO <sub>2</sub> Thin Films: Photocatalytic and Bactericidal Activity. ACS Applied Materials & Interfaces, 2021, 13, 10480-10489.	8.0	28
36	Multifunctional two-dimensional glassy graphene devices for vis-NIR photodetection and volatile organic compound sensing. Science China Materials, 2021, 64, 1964-1976.	6.3	5

#	Article	IF	CITATIONS
37	Optimization of the thermochromic glazing design for curtain wall buildings based on experimental measurements and dynamic simulation. Solar Energy, 2021, 216, 14-25.	6.1	23
38	Multivalent Ion Batteries: Cathode Design for Aqueous Rechargeable Multivalent Ion Batteries: Challenges and Opportunities (Adv. Funct. Mater. 13/2021). Advanced Functional Materials, 2021, 31, 2170089.	14.9	1
39	Natural Clayâ€Based Materials for Energy Storage and Conversion Applications. Advanced Science, 2021, 8, e2004036.	11.2	56
40	Modelling and measurement of laser-generated focused ultrasound: Can interventional transducers achieve therapeutic effects?. Journal of the Acoustical Society of America, 2021, 149, 2732-2742.	1.1	2
41	Insights on Flexible Zincâ€lon Batteries from Lab Research to Commercialization. Advanced Materials, 2021, 33, e2007548.	21.0	191
42	A coating-free superhydrophobic sensing material for full-range human motion and microliter droplet impact detection. Chemical Engineering Journal, 2021, 410, 128418.	12.7	22
43	Zincâ€lon Batteries: Insights on Flexible Zincâ€lon Batteries from Lab Research to Commercialization (Adv.) Tj l	TQq1 1 0.1 21.0	784314 rgBT
44	Enhancing Hydrogen Evolution Electrocatalytic Performance in Neutral Media via Nitrogen and Iron Phosphide Interactions. Small Science, 2021, 1, 2100032.	9.9	24
45	High Surface Area of Polyhedral Chromia and Hexagonal Chromium Sulfide by the Thermolysis of Cyclohexylammonium Hexaisothiocyanatochromate(III) Sesquihydrate. ChemistrySelect, 2021, 6, 4298-4311.	1.5	2
46	Generating, probing and utilising photo-induced surface oxygen vacancies for trace molecular detection. , 2021, , .		0
47	Robust Protection of III–V Nanowires in Water Splitting by a Thin Compact TiO <sub>2</sub> Layer. ACS Applied Materials & Interfaces, 2021, 13, 30950-30958.	8.0	12
48	Delayed Lubricant Depletion of Slippery Liquid Infused Porous Surfaces Using Precision Nanostructures. Langmuir, 2021, 37, 10071-10078.	3.5	31
49	Magnetic Field-Induced Orientation of Modified Boron Nitride Nanosheets in Epoxy Resin with Improved Flame and Wear Resistance. Langmuir, 2021, 37, 8222-8231.	3.5	12
50	Facile Fabrication of Robust Hydrogen Evolution Electrodes under High Current Densities via Pt@Cu Interactions. Advanced Functional Materials, 2021, 31, 2105579.	14.9	45
51	Flame retardant and superhydrophobic composites via oriented arrangement of boron nitride nanosheets. Journal of Materials Science, 2021, 56, 19955-19968.	3.7	1
52	The Effect of Photoinduced Surface Oxygen Vacancies on the Charge Carrier Dynamics in TiO <sub>2</sub> Films. Nano Letters, 2021, 21, 8348-8354.	9.1	29
53	Engineering Polymer Glue towards 90% Zinc Utilization for 1000 Hours to Make Highâ€Performance Znâ€Ion Batteries. Advanced Functional Materials, 2021, 31, 2107652.	14.9	115
54	Bioinspired Multifunctional Glass Surfaces through Regenerative Secondary Mask Lithography. Advanced Materials, 2021, 33, e2102175.	21.0	13

#	Article	IF	CITATIONS
55	CulnS <sub>2</sub> Quantum Dot and Polydimethylsiloxane Nanocomposites for Allâ€Optical Ultrasound and Photoacoustic Imaging. Advanced Materials Interfaces, 2021, 8, 2100518.	3.7	13
56	Kinetics-based design of a flow platform for highly reproducible on demand synthesis of gold nanoparticles with controlled size between 50 and 150Ânm and their application in SERS and PIERS sensing. Chemical Engineering Journal, 2021, 423, 129069.	12.7	13
5 <b>7</b>	A study of the interaction of cationic dyes with gold nanostructures. RSC Advances, 2021, 11, 17694-17703.	3.6	1
58	Cathode Design for Aqueous Rechargeable Multivalent Ion Batteries: Challenges and Opportunities. Advanced Functional Materials, 2021, 31, 2010445.	14.9	102
59	SERS multiplexing of methylxanthine drug isomers <i>via</i> host–guest size matching and machine learning. Journal of Materials Chemistry C, 2021, 9, 12624-12632.	5.5	15
60	Crystal Violet-Impregnated Slippery Surface to Prevent Bacterial Contamination of Surfaces. ACS Applied Materials & Interfaces, 2021, 13, 5478-5485.	8.0	12
61	Investigation of a Biomass Hydrogel Electrolyte Naturally Stabilizing Cathodes for Zinc-Ion Batteries. ACS Applied Materials & Interfaces, 2021, 13, 745-754.	8.0	64
62	CuInS <sub>2</sub> Quantum Dot and Polydimethylsiloxane Nanocomposites for Allâ€Optical Ultrasound and Photoacoustic Imaging (Adv. Mater. Interfaces 20/2021). Advanced Materials Interfaces, 2021, 8, 2170114.	3.7	0
63	Rechargeable aqueous Zn-based energy storage devices. Joule, 2021, 5, 2845-2903.	24.0	201
64	Probing the Role of Atomic Defects in Photocatalytic Systems through Photoinduced Enhanced Raman Scattering. ACS Energy Letters, 2021, 6, 4273-4281.	17.4	22
65	Superhydrophilic–superhydrophobic patterned surfaces on glass substrate for water harvesting. Journal of Materials Science, 2020, 55, 498-508.	3.7	46
66	Resonant doping for high mobility transparent conductors: the case of Mo-doped In <sub>2</sub> O <sub>3</sub> . Materials Horizons, 2020, 7, 236-243.	12.2	64
67	Rapid synthesis of [Au25(Cys)18] nanoclusters via carbon monoxide in microfluidic liquid-liquid segmented flow system and their antimicrobial performance. Chemical Engineering Journal, 2020, 383, 123176.	12.7	18
68	Oxygen vacancy engineering in spinel-structured nanosheet wrapped hollow polyhedra for electrochemical nitrogen fixation under ambient conditions. Journal of Materials Chemistry A, 2020, 8, 1652-1659.	10.3	59
69	Room Temperature Synthesis of Phosphineâ€Capped Lead Bromide Perovskite Nanocrystals without Coordinating Solvents. Particle and Particle Systems Characterization, 2020, 37, 1900391.	2.3	27
70	Corrosion of One-Step Superhydrophobic Stainless-Steel Thermal Spray Coatings. ACS Applied Materials & Interfaces, 2020, 12, 1523-1532.	8.0	33
71	Ambipolar and Robust WSe 2 Fieldâ€Effect Transistors Utilizing Selfâ€Assembled Edge Oxides. Advanced Materials Interfaces, 2020, 7, 1901628.	3.7	11
72	Continuous Single-Phase Synthesis of [Au25(Cys)18] Nanoclusters and their Photobactericidal Enhancement. ACS Applied Materials & Interfaces, 2020, 12, 49021-49029.	8.0	7

#	Article	IF	CITATIONS
73	Enabling stable MnO <sub>2</sub> matrix for aqueous zinc-ion battery cathodes. Journal of Materials Chemistry A, 2020, 8, 22075-22082.	10.3	101
74	Nonmonotonic contactless manipulation of binary droplets via sensing of localized vapor sources on pristine substrates. Science Advances, 2020, 6, .	10.3	19
75	Flexible and Strong Robust Superhydrophobic Monoliths with Antibacterial Property. ACS Applied Polymer Materials, 2020, 2, 4856-4863.	4.4	22
76	Antimicrobial surfaces: A need for stewardship?. PLoS Pathogens, 2020, 16, e1008880.	4.7	22
77	A Hierarchical 3D TiO <sub>2</sub> /Ni Nanostructure as an Efficient Holeâ€Extraction and Protection Layer for GaAs Photoanodes. ChemSusChem, 2020, 13, 6028-6036.	6.8	8
78	Probing Mg Intercalation in the Tetragonal Tungsten Bronze Framework V <sub>4</sub> Nb <sub>18</sub> O <sub>55</sub> . Inorganic Chemistry, 2020, 59, 9783-9797.	4.0	7
79	Recent Developments in the Field of Explosive Trace Detection. ACS Nano, 2020, 14, 10804-10833.	14.6	110
80	Qualitative Approaches Towards Useful Photocatalytic Materials. Frontiers in Chemistry, 2020, 8, 817.	3.6	5
81	Probing the electronic and geometric structures of photoactive electrodeposited Cu2O films by X-ray absorption spectroscopy. Journal of Catalysis, 2020, 389, 483-491.	6.2	8
82	An anti-aging polymer electrolyte for flexible rechargeable zinc-ion batteries. Journal of Materials Chemistry A, 2020, 8, 22637-22644.	10.3	41
83	Cocaine by-product detection with metal oxide semiconductor sensor arrays. RSC Advances, 2020, 10, 28464-28477.	3.6	6
84	Spacer-Defined Intrinsic Multiple Patterning. ACS Nano, 2020, 14, 12091-12100.	14.6	10
85	High-Performance Zinc–Air Batteries with Scalable Metal–Organic Frameworks and Platinum Carbon Black Bifunctional Catalysts. ACS Applied Materials & Interfaces, 2020, 12, 42696-42703.	8.0	41
86	Thermoresponsive Black VO2–Carbon Nanotube Composite Coatings for Solar Energy Harvesting. ACS Applied Nano Materials, 2020, 3, 8848-8857.	5.0	8
87	Combined Effect of Temperature Induced Strain and Oxygen Vacancy on Metalâ€Insulator Transition of VO <sub>2</sub> Colloidal Particles. Advanced Functional Materials, 2020, 30, 2005311.	14.9	42
88	Particle Size Evolution during the Synthesis of Gold Nanoparticles Using <i>In Situ</i> Time-Resolved UV–Vis Spectroscopy: An Experimental and Theoretical Study Unravelling the Effect of Adsorbed Gold Precursor Species. Journal of Physical Chemistry C, 2020, 124, 27662-27672.	3.1	11
89	Fluorine-Free Transparent Superhydrophobic Nanocomposite Coatings from Mesoporous Silica. Langmuir, 2020, 36, 13426-13438.	3.5	31
90	Synergistic interactions of cadmium-free quantum dots embedded in a photosensitised polymer surface: efficient killing of multidrug-resistant strains at low ambient light levels. Nanoscale, 2020, 12, 10609-10622.	5.6	6

#	Article	IF	CITATIONS
91	Dual-triggered nanoaggregates of cucurbit[7]uril and gold nanoparticles for multi-spectroscopic quantification of creatinine in urinalysis. Journal of Materials Chemistry C, 2020, 8, 7051-7058.	5.5	16
92	N <sub>2</sub> Electroreduction to NH <sub>3</sub> by Selenium Vacancyâ€Rich ReSe <sub>2</sub> Catalysis at an Abrupt Interface. Angewandte Chemie - International Edition, 2020, 59, 13320-13327.	13.8	127
93	Effective onâ€line highâ€speed shear dispersing emulsifier technique coupled with highâ€performance countercurrent chromatography method for simultaneous extraction and isolation ofAcarotenoids from <i>Lycium barbarum</i> L. fruits. Journal of Separation Science, 2020, 43, 2949-2958.	2.5	9
94	N <sub>2</sub> Electroreduction to NH <sub>3</sub> by Selenium Vacancyâ€Rich ReSe <sub>2</sub> Catalysis at an Abrupt Interface. Angewandte Chemie, 2020, 132, 13422-13429.	2.0	18
95	New Insights into the Fundamental Principle of Semiconductor Photocatalysis. ACS Omega, 2020, 5, 14847-14856.	3.5	44
96	Advances towards programmable droplet transport on solid surfaces and its applications. Chemical Society Reviews, 2020, 49, 7879-7892.	38.1	86
97	Controlling the Thermoelectric Properties of Organometallic Coordination Polymers via Ligand Design. Advanced Functional Materials, 2020, 30, 2003106.	14.9	15
98	Highly reproducible, high-yield flow synthesis of gold nanoparticles based on a rational reactor design exploiting the reduction of passivated Au( <scp>iii</scp> ). Reaction Chemistry and Engineering, 2020, 5, 663-676.	3.7	33
99	Microstructure and antibacterial efficacy of graphene oxide nanocomposite fibres. Journal of Colloid and Interface Science, 2020, 571, 239-252.	9.4	67
100	Radio-metal cross-linking of alginate hydrogels for non-invasive in vivo imaging. Biomaterials, 2020, 243, 119930.	11.4	29
101	Antibacterial Surfaces with Activity against Antimicrobial Resistant Bacterial Pathogens and Endospores. ACS Infectious Diseases, 2020, 6, 939-946.	3.8	21
102	Photobactericidal activity activated by thiolated gold nanoclusters at low flux levels of white light. Nature Communications, 2020, 11, 1207.	12.8	52
103	Following the Formation of Silver Nanoparticles Using <i>In Situ</i> X-ray Absorption Spectroscopy. ACS Omega, 2020, 5, 13664-13671.	3.5	8
104	Nanostructured titanium dioxide coatings prepared by Aerosol Assisted Chemical Vapour Deposition (AACVD). Journal of Photochemistry and Photobiology A: Chemistry, 2020, 400, 112727.	3.9	20
105	Defected vanadium bronzes as superb cathodes in aqueous zinc-ion batteries. Nanoscale, 2020, 12, 20638-20648.	5.6	61
106	Self-healing on mismatched fractured composite surfaces of SiC with a diameter of 180 nm. Nanoscale, 2020, 12, 19617-19627.	5.6	3
107	Aerosol-assisted route to low-E transparent conductive gallium-doped zinc oxide coatings from pre-organized and halogen-free precursor. Chemical Science, 2020, 11, 4980-4990.	7.4	12
108	Multi‣cale Investigations of δâ€Ni <sub>0.25</sub> V <sub>2</sub> O <sub>5</sub> ·nH <sub>2</sub> O Cathode Materials in Aqueous Zincâ€ion Batteries. Advanced Energy Materials, 2020, 10, 2000058.	19.5	173

#	Article	IF	CITATIONS
109	Macroscale Superlubricity: Macroscale Superlubricity Enabled by Grapheneâ€Coated Surfaces (Adv. Sci.) Tj ETQq1	10,78431 11.2	14 rgBT /0\
110	Tuning the interlayer spacing of graphene laminate films for efficient pore utilization towards compact capacitive energy storage. Nature Energy, 2020, 5, 160-168.	39.5	381
111	Resonant Ta Doping for Enhanced Mobility in Transparent Conducting SnO <sub>2</sub> . Chemistry of Materials, 2020, 32, 1964-1973.	6.7	50
112	Enhanced Photocatalytic and Antibacterial Ability of Cu-Doped Anatase TiO <sub>2</sub> Thin Films: Theory and Experiment. ACS Applied Materials & Interfaces, 2020, 12, 15348-15361.	8.0	102
113	Adsorption of volatile organic compounds by industrial porous materials: Impact of relative humidity. Microporous and Mesoporous Materials, 2020, 298, 110090.	4.4	47
114	Highly conductive and transparent gallium doped zinc oxide thin films via chemical vapor deposition. Scientific Reports, 2020, 10, 638.	3.3	102
115	Refining Energy Levels in ReS <sub>2</sub> Nanosheets by Lowâ€Valent Transitionâ€Metal Doping for Dualâ€Boosted Electrochemical Ammonia/Hydrogen Production. Advanced Functional Materials, 2020, 30, 1907376.	14.9	99
116	High-Performance Planar Thin Film Thermochromic Window via Dynamic Optical Impedance Matching. ACS Applied Materials & Interfaces, 2020, 12, 8140-8145.	8.0	22
117	Macroscale Superlubricity Enabled by Graphene oated Surfaces. Advanced Science, 2020, 7, 1903239.	11.2	64
118	The applicability of high-speed counter current chromatography to the separation of natural antioxidants. Journal of Chromatography A, 2020, 1623, 461150.	3.7	54
119	Charge carrier transfer in photocatalysis. Interface Science and Technology, 2020, , 103-159.	3.3	2
120	The Role of Phosphate Group in Doped Cobalt Molybdate: Improved Electrocatalytic Hydrogen Evolution Performance. Advanced Science, 2020, 7, 1903674.	11.2	73
121	Flexible and Selfâ€Powered Photodetector Arrays Based on Allâ€Inorganic CsPbBr <sub>3</sub> Quantum Dots. Advanced Materials, 2020, 32, e2000004.	21.0	134
122	Zincâ€ŀon Batteries: Multi‧cale Investigations of δâ€Ni <sub>0.25</sub> V <sub>2</sub> O <sub>5</sub> ·nH <sub>2</sub> O Cathode Materials in Aqueous Zincâ€ŀon Batteries (Adv. Energy Mater. 15/2020). Advanced Energy Materials, 2020, 10, 2070068.	19.5	8
123	Ultra high molecular weight polyethylene with incorporated crystal violet and gold nanoclusters is antimicrobial in low intensity light and in the dark. Materials Advances, 2020, 1, 3339-3348.	5.4	3
124	Quantitative SERS Detection of Uric Acid via Formation of Precise Plasmonic Nanojunctions within Aggregates of Gold Nanoparticles and Cucurbit[ <em>n</em> ]uril. Journal of Visualized Experiments, 2020, , .	0.3	1
125	Unprecedented Piezoresistance Coefficient in Strained Silicon Carbide. Nano Letters, 2019, 19, 6569-6576.	9.1	62
126	Influence of Lithium and Lanthanum Treatment on TiO 2 Nanofibers and Their Application in nâ€iâ€p Solar Cells. ChemElectroChem, 2019, 6, 3529-3529.	3.4	0

#	Article	IF	CITATIONS
127	Fabrication of robust superhydrophobic surfaces <i>via</i> aerosol-assisted CVD and thermo-triggered healing of superhydrophobicity by recovery of roughness structures. Journal of Materials Chemistry A, 2019, 7, 17604-17612.	10.3	91
128	Dual-scale TiO <sub>2</sub> and SiO <sub>2</sub> particles in combination with a fluoroalkylsilane and polydimethylsiloxane superhydrophobic/superoleophilic coating for efficient solvent–water separation. RSC Advances, 2019, 9, 20332-20340.	3.6	11
129	Slippery Liquid Infused Porous TiO <sub>2</sub> /SnO <sub>2</sub> Nanocomposite Thin Films via Aerosol Assisted Chemical Vapor Deposition with Anti-Icing and Fog Retardant Properties. ACS Applied Materials & Interfaces, 2019, 11, 41804-41812.	8.0	38
130	Modifying Epoxy Resins to Resist Both Fire and Water. Langmuir, 2019, 35, 14332-14338.	3.5	12
131	Differential Phagocytosis-Based Photothermal Ablation of Inflammatory Macrophages in Atherosclerotic Disease. ACS Applied Materials & Interfaces, 2019, 11, 41009-41018.	8.0	33
132	Fabrication and characterization of degradable and durable fluoride-free super-hydrophobic cotton fabrics for oil/water separation. Surface and Coatings Technology, 2019, 378, 125079.	4.8	35
133	Robust Superhydrophobic Conical Pillars from Syringe Needle Shape to Straight Conical Pillar Shape for Droplet Pancake Bouncing. ACS Applied Materials & Interfaces, 2019, 11, 45345-45353.	8.0	56
134	Dynamics of Photoâ€Induced Surface Oxygen Vacancies in Metalâ€Oxide Semiconductors Studied Under Ambient Conditions. Advanced Science, 2019, 6, 1901841.	11.2	62
135	Carboxylic Acid Functionalization at the Meso-Position of the Bodipy Core and Its Influence on Photovoltaic Performance. Nanomaterials, 2019, 9, 1346.	4.1	3
136	Gaseous Photocatalytic Oxidation of Formic Acid over TiO <sub>2</sub> : A Comparison between the Charge Carrier Transfer and Light-Assisted Mars–van Krevelen Pathways. Journal of Physical Chemistry C, 2019, 123, 22261-22272.	3.1	13
137	Super-robust superamphiphobic surface with anti-icing property. RSC Advances, 2019, 9, 27702-27709.	3.6	14
138	Surface radio-mineralisation mediates chelate-free radiolabelling of iron oxide nanoparticles. Chemical Science, 2019, 10, 2592-2597.	7.4	15
139	<i>In vivo</i> and <i>in vitro</i> efficient textile wastewater remediation by <i>Aspergillus niger</i> biosorbent. Nanoscale Advances, 2019, 1, 168-176.	4.6	35
140	Oneâ€step synthesis of Ag@PS nanospheres via flash nanoprecipitation. Applied Organometallic Chemistry, 2019, 33, e4713.	3.5	6
141	Influence of Humidity on the NO2 Sensing Properties of SrCo0.1Ti0.9O3. Springer Proceedings in Physics, 2019, , 905-911.	0.2	0
142	Origin of High-Efficiency Photoelectrochemical Water Splitting on Hematite/Functional Nanohybrid Metal Oxide Overlayer Photoanode after a Low Temperature Inert Gas Annealing Treatment. ACS Omega, 2019, 4, 1449-1459.	3.5	20
143	Heterojunction αâ€Fe <sub>2</sub> O <sub>3</sub> /ZnO Films with Enhanced Photocatalytic Properties Grown by Aerosolâ€Assisted Chemical Vapour Deposition. Chemistry - A European Journal, 2019, 25, 11337-11345 Thermochromic <mml:math <="" td="" xmlns:mml="http://www.w3.org/1998/Math/MathML"><td>3.3</td><td>28</td></mml:math>	3.3	28
144	altimg="si1.svg"> <mml:mrow><mml:msub><mml:mrow><mml:mtext>VO</mml:mtext></mml:mrow><mml:n linebreak="goodbreak" linebreakstyle="after"&gt;â^'<mml:msub><mml:mrow><mml:mtext>SiO</mml:mtext></mml:mrow>&lt; nanocomposite smart window coatings with narrow phase transition hysteresis and transition gradient width. Solar Energy Materials and Solar Cells, 2019, 200, 109944.</mml:msub></mml:n </mml:msub></mml:mrow>		

#	Article	IF	CITATIONS
145	Aerosol-assisted chemical vapour deposition of transparent superhydrophobic film by using mixed functional alkoxysilanes. Scientific Reports, 2019, 9, 7549.	3.3	41
146	Application of levitation-jet synthesized nickel-based nanoparticles for gas sensing. Materials Science and Engineering B: Solid-State Materials for Advanced Technology, 2019, 244, 81-92.	3.5	12
147	Ultrahigh Recovery of Fracture Strength on Mismatched Fractured Amorphous Surfaces of Silicon Carbide. ACS Nano, 2019, 13, 7483-7492.	14.6	54
148	Origin of Performance Enhancement in TiO <sub>2</sub> arbon Nanotube Composite Perovskite Solar Cells. Small Methods, 2019, 3, 1900164.	8.6	45
149	Continuous separation of maslinic and oleanolic acids from olive pulp by highâ€speed countercurrent chromatography with elutionâ€extrusion mode. Journal of Separation Science, 2019, 42, 2080-2088.	2.5	18
150	High-efficiency bubble transportation in an aqueous environment on a serial wedge-shaped wettability pattern. Journal of Materials Chemistry A, 2019, 7, 13567-13576.	10.3	90
151	Selective Detection of Nitroexplosives Using Molecular Recognition within Self-Assembled Plasmonic Nanojunctions. Journal of Physical Chemistry C, 2019, 123, 15769-15776.	3.1	31
152	Reactive silica nanoparticles turn epoxy coating from hydrophilic to super-robust superhydrophobic. RSC Advances, 2019, 9, 12547-12554.	3.6	28
153	High Defect Nanoscale ZnO Films with Polar Facets for Enhanced Photocatalytic Performance. ACS Applied Nano Materials, 2019, 2, 2881-2889.	5.0	29
154	A rugged, self-sterilizing antimicrobial copper coating on ultra-high molecular weight polyethylene: a preliminary study on the feasibility of an antimicrobial prosthetic joint material. Journal of Materials Chemistry B, 2019, 7, 3310-3318.	5.8	14
155	Dispelling the Myth of Passivated Codoping in TiO <sub>2</sub> . Chemistry of Materials, 2019, 31, 2577-2589.	6.7	17
156	Sensing and Discrimination of Explosives at Variable Concentrations with a Large-Pore MOF as Part of a Luminescent Array. ACS Applied Materials & 2019, 11, 11618, 11618, 11626.	8.0	54
157	Intrinsic intermediate gap states of TiO2 materials and their roles in charge carrier kinetics. Journal of Photochemistry and Photobiology C: Photochemistry Reviews, 2019, 39, 1-57.	11.6	70
158	Functionalised iron oxide nanoparticles for multimodal optoacoustic and magnetic resonance imaging. Journal of Materials Chemistry B, 2019, 7, 2212-2219.	5.8	15
159	Photoactivable Polymers Embedded with Cadmium-Free Quantum Dots and Crystal Violet: Efficient Bactericidal Activity against Clinical Strains of Antibiotic-Resistant Bacteria. ACS Applied Materials & Interfaces, 2019, 11, 12367-12378.	8.0	30
160	Heteroepitaxy of GaP on silicon for efficient and cost-effective photoelectrochemical water splitting. Journal of Materials Chemistry A, 2019, 7, 8550-8558.	10.3	19
161	Influence of Lithium and Lanthanum Treatment on TiO 2 Nanofibers and Their Application in nâ€iâ€p Solar Cells. ChemElectroChem, 2019, 6, 3590-3598.	3.4	5
162	All-Optical Rotational Ultrasound Imaging. Scientific Reports, 2019, 9, 5576.	3.3	47

#	Article	IF	CITATIONS
163	Cucurbituril-mediated quantum dot aggregates formed by aqueous self-assembly for sensing applications. Chemical Communications, 2019, 55, 5495-5498.	4.1	11
164	Rapid synthesis of gold nanoparticles with carbon monoxide in a microfluidic segmented flow system. Reaction Chemistry and Engineering, 2019, 4, 884-890.	3.7	35
165	Photoelectrochemical water oxidation of GaP <sub>1â^'x</sub> Sb <sub>x</sub> with a direct band gap of 1.65 eV for full spectrum solar energy harvesting. Sustainable Energy and Fuels, 2019, 3, 1720-1729.	4.9	14
166	Enhanced performance of ZnO nanoparticle decorated all-inorganic CsPbBr <sub>3</sub> quantum dot photodetectors. Journal of Materials Chemistry A, 2019, 7, 6134-6142.	10.3	64
167	Thermally-induced all-damage-healable superhydrophobic surface with photocatalytic performance from hierarchical BiOCl. Chemical Engineering Journal, 2019, 366, 439-448.	12.7	37
168	Surface Oxygen Vacancies: Dynamics of Photoâ€Induced Surface Oxygen Vacancies in Metalâ€Oxide Semiconductors Studied Under Ambient Conditions (Adv. Sci. 22/2019). Advanced Science, 2019, 6, 1970132.	11.2	3
169	New Insight into the Role of Electron Transfer to O <sub>2</sub> in Photocatalytic Oxidations of Acetone over TiO <sub>2</sub> and the Effect of Au Cocatalyst. Journal of Physical Chemistry C, 2019, 123, 30958-30971.	3.1	16
170	Energy level engineering in transition-metal doped spinel-structured nanosheets for efficient overall water splitting. Journal of Materials Chemistry A, 2019, 7, 827-833.	10.3	52
171	Exceptional supercapacitor performance from optimized oxidation of graphene-oxide. Energy Storage Materials, 2019, 17, 12-21.	18.0	135
172	Photo-induced enhanced Raman spectroscopy (PIERS): sensing atomic-defects, explosives and biomolecules. , 2019, , .		2
173	Controlling and modelling the wetting properties of III-V semiconductor surfaces using re-entrant nanostructures. Scientific Reports, 2018, 8, 3544.	3.3	4
174	Robust platform for water harvesting and directional transport. Journal of Materials Chemistry A, 2018, 6, 5635-5643.	10.3	71
175	Chemically Treated 3D Printed Polymer Scaffolds for Biomineral Formation. ACS Omega, 2018, 3, 4342-4351.	3.5	24
176	A Dendritic Nickel Cobalt Sulfide Nanostructure for Alkaline Battery Electrodes. Advanced Functional Materials, 2018, 28, 1705937.	14.9	138
177	The Effect of Alkali Metal (Na, K) Doping on Thermochromic Properties of VO2 Films. MRS Advances, 2018, 3, 1863-1869.	0.9	5
178	Chemical Vapor Deposition of Photocatalytically Active Pure Brookite TiO <sub>2</sub> Thin Films. Chemistry of Materials, 2018, 30, 1353-1361.	6.7	79
179	Dynamic Control of Particle Deposition in Evaporating Droplets by an External Point Source of Vapor. Journal of Physical Chemistry Letters, 2018, 9, 659-664.	4.6	58
180	Deeper Understanding of Interstitial Boron-Doped Anatase Thin Films as A Multifunctional Layer Through Theory and Experiment. Journal of Physical Chemistry C, 2018, 122, 714-726.	3.1	16

#	Article	IF	CITATIONS
181	A superhydrophilic cement-coated mesh: an acid, alkali, and organic reagent-free material for oil/water separation. Nanoscale, 2018, 10, 1920-1929.	5.6	81
182	Polydimethylsiloxane Composites for Optical Ultrasound Generation and Multimodality Imaging. Advanced Functional Materials, 2018, 28, 1704919.	14.9	81
183	Synergistic relationship between the three-dimensional nanostructure and electrochemical performance in biocarbon supercapacitor electrode materials. Sustainable Energy and Fuels, 2018, 2, 772-785.	4.9	53
184	Aluminium/gallium, indium/gallium, and aluminium/indium co-doped ZnO thin films deposited <i>via</i> aerosol assisted CVD. Journal of Materials Chemistry C, 2018, 6, 588-597.	5.5	72
185	White-Light-Activated Antibacterial Surfaces Generated by Synergy between Zinc Oxide Nanoparticles and Crystal Violet. ACS Omega, 2018, 3, 3190-3199.	3.5	25
186	Computational Intelligenceâ€Assisted Understanding of Natureâ€Inspired Superhydrophobic Behavior. Advanced Science, 2018, 5, 1700520.	11.2	19
187	Covalently Attached Antimicrobial Surfaces Using BODIPY: Improving Efficiency and Effectiveness. ACS Applied Materials & Interfaces, 2018, 10, 98-104.	8.0	35
188	High efficiency water splitting photoanodes composed of nano-structured anatase-rutile TiO2 heterojunctions by pulsed-pressure MOCVD. Applied Catalysis B: Environmental, 2018, 224, 904-911.	20.2	51
189	Super-durable, non-fluorinated superhydrophobic free-standing items. Journal of Materials Chemistry A, 2018, 6, 357-362.	10.3	75
190	Elucidating iron doping induced n- to p- characteristics of Strontium titanate based ethanol sensors. Current Applied Physics, 2018, 18, 246-253.	2.4	11
191	Room temperature vanadium dioxide–carbon nanotube gas sensors made via continuous hydrothermal flow synthesis. Sensors and Actuators B: Chemical, 2018, 255, 1119-1129.	7.8	57
192	A new family of urea-based low molecular-weight organogelators for environmental remediation: the influence of structure. Soft Matter, 2018, 14, 8821-8827.	2.7	11
193	Direct and continuous hydrothermal flow synthesis of thermochromic phase pure monoclinic VO <sub>2</sub> nanoparticles. Journal of Materials Chemistry C, 2018, 6, 11731-11739.	5.5	15
194	Effects of bovine serum albumin on light activated antimicrobial surfaces. RSC Advances, 2018, 8, 34252-34258.	3.6	9
195	The effect of solvent on Al-doped ZnO thin films deposited <i>via</i> aerosol assisted CVD. RSC Advances, 2018, 8, 33164-33173.	3.6	39
196	Single step route to highly transparent, conductive and hazy aluminium doped zinc oxide films. RSC Advances, 2018, 8, 42300-42307.	3.6	28
197	Synthesis of superhydrophobic surfaces with Wenzel and Cassie–Baxter state: experimental evidence and theoretical insight. Nanotechnology, 2018, 29, 485601.	2.6	17
198	Characterisation of VOCs Surrounding Naum Gabo's <i>Construction in Space â€~Two Cones</i> ', (Tate) by <i>in situ</i> SPME GC-MS Monitoring. Studies in Conservation, 2018, 63, 369-371.	1.1	10

#	Article	IF	CITATIONS
199	InGaN/GaN Multiple Quantum Well Photoanode Modified with Cobalt Oxide for Water Oxidation. ACS Applied Energy Materials, 2018, 1, 6417-6424.	5.1	23
200	Multifunctional Porous and Magnetic Silicone with High Elasticity, Durability, and Oil–Water Separation Properties. Langmuir, 2018, 34, 13305-13311.	3.5	25
201	Mitigation of hysteresis due to a pseudo-photochromic effect in thermochromic smart window coatings. Scientific Reports, 2018, 8, 13249.	3.3	11
202	Cobalt nickel nitride coated by a thin carbon layer anchoring on nitrogen-doped carbon nanotube anodes for high-performance lithium-ion batteries. Journal of Materials Chemistry A, 2018, 6, 19853-19862.	10.3	38
203	Solid solution nitride/carbon nanotube hybrids enhance electrocatalysis of oxygen in zinc-air batteries. Energy Storage Materials, 2018, 15, 380-387.	18.0	32
204	The Anti-Biofouling Properties of Superhydrophobic Surfaces are Short-Lived. ACS Nano, 2018, 12, 6050-6058.	14.6	222
205	Luminescence behaviour and deposition of Sc2O3 thin films from scandium(III) acetylacetonate at ambient pressure. Applied Physics Letters, 2018, 112, 221902.	3.3	11
206	57Fe Mössbauer study of NiFe2O4 nanoparticles produced by the levitation-jet aerosol technique. Journal of Materials Science: Materials in Electronics, 2018, 29, 14347-14352.	2.2	1
207	Encapsulation of metal precursor within ZIFs for bimetallic N-doped carbon electrocatalyst with enhanced oxygen reduction. International Journal of Hydrogen Energy, 2018, 43, 14701-14709.	7.1	26
208	Enhanced electrical properties of antimony doped tin oxide thin films deposited <i>via</i> aerosol assisted chemical vapour deposition. Journal of Materials Chemistry C, 2018, 6, 7257-7266.	5.5	97
209	Photobactericidal Activity of Dual Dyes Encapsulated in Silicone Enhanced by Silver Nanoparticles. ACS Omega, 2018, 3, 6779-6786.	3.5	8
210	Inexpensive and non-toxic water repellent coatings comprising SiO <sub>2</sub> nanoparticles and long chain fatty acids. RSC Advances, 2018, 8, 27064-27072.	3.6	26
211	Video-rate all-optical ultrasound imaging. Biomedical Optics Express, 2018, 9, 3481.	2.9	25
212	Nb-doped rutile titanium dioxide nanorods for lithium-ion batteries. Solid State Sciences, 2018, 83, 115-121.	3.2	20
213	Sulfurâ€Deficient Bismuth Sulfide/Nitrogenâ€Doped Carbon Nanofibers as Advanced Freeâ€Standing Electrode for Asymmetric Supercapacitors. Small, 2018, 14, e1801562.	10.0	117
214	Reflective Silver Thin Film Electrodes from Commercial Silver(I) Triflate via Aerosol-Assisted Chemical Vapor Deposition. ACS Applied Nano Materials, 2018, 1, 3724-3732.	5.0	6
215	Integration of supercapacitors into printed circuit boards. Journal of Energy Storage, 2018, 19, 28-34.	8.1	14
216	Efficiently texturing hierarchical superhydrophobic fluoride-free translucent films by AACVD with excellent durability and self-cleaning ability. Journal of Materials Chemistry A, 2018, 6, 17633-17641.	10.3	99

#	Article	IF	CITATIONS
217	Evaluation of the BET Theory for the Characterization of Meso and Microporous MOFs. Small Methods, 2018, 2, 1800173.	8.6	288
218	Battery Electrodes: A Dendritic Nickel Cobalt Sulfide Nanostructure for Alkaline Battery Electrodes (Adv. Funct. Mater. 23/2018). Advanced Functional Materials, 2018, 28, 1870154.	14.9	7
219	Photocatalytic and electrically conductive transparent Cl-doped ZnO thin films <i>via</i> aerosol-assisted chemical vapour deposition. Journal of Materials Chemistry A, 2018, 6, 12682-12692.	10.3	34
220	Tuning operating temperature of BaSnO3 gas sensor for reducing and oxidizing gases. AIP Conference Proceedings, 2018, , .	0.4	4
221	Continuous flow synthesis of ultrasmall gold nanoparticles in a microreactor using trisodium citrate and their SERS performance. Chemical Engineering Science, 2018, 189, 422-430.	3.8	68
222	A combined experimental and theoretical study into the performance of multilayer vanadium dioxide nanocomposites for energy saving applications. , 2018, , .		3
223	Light-driven generation of chlorine and hydrogen from brine using highly selective Ru/Ti oxide redox catalysts. Sustainable Energy and Fuels, 2017, 1, 254-257.	4.9	3
224	Ultrasmall CuCo <sub>2</sub> S <sub>4</sub> Nanocrystals: Allâ€inâ€One Theragnosis Nanoplatform with Magnetic Resonance/Nearâ€Infrared Imaging for Efficiently Photothermal Therapy of Tumors. Advanced Functional Materials, 2017, 27, 1606218.	14.9	106
225	Ultraviolet Radiation Induced Dopant Loss in a TiO <sub>2</sub> Photocatalyst. ACS Catalysis, 2017, 7, 1485-1490.	11.2	18
226	Structure of Gold–Silver Nanoparticles. Journal of Physical Chemistry C, 2017, 121, 1957-1963.	3.1	36
227	A Comparison of the Potential Capability of SFS, SPS and HVSFS for the Production of Photocatalytic Titania Coatings. Journal of Thermal Spray Technology, 2017, 26, 161-172.	3.1	3
228	Nanocellulose crystals derivative-silica hybrid sol open tubular capillary column for enantioseparation. Carbohydrate Polymers, 2017, 165, 359-367.	10.2	20
229	One-step constrained-volume synthesis of silver decorated polymer colloids with antimicrobial and sensing properties. Colloid and Polymer Science, 2017, 295, 521-527.	2.1	12
230	Transparent conducting oxide thin films of Si-doped ZnO prepared by aerosol assisted CVD. RSC Advances, 2017, 7, 10806-10814.	3.6	36
231	High-Throughput Continuous Hydrothermal Synthesis of Transparent Conducting Aluminum and Gallium Co-doped Zinc Oxides. ACS Combinatorial Science, 2017, 19, 239-245.	3.8	17
232	Optimizing the Activity of Nanoneedle Structured WO <sub>3</sub> Photoanodes for Solar Water Splitting: Direct Synthesis via Chemical Vapor Deposition. Journal of Physical Chemistry C, 2017, 121, 5983-5993.	3.1	71
233	Enhancing the Magnetic Heating Capacity of Iron Oxide Nanoparticles through Their Postproduction Incorporation into Iron Oxide–Gold Nanocomposites. European Journal of Inorganic Chemistry, 2017, 2017, 2386-2395.	2.0	11
234	Continuous flow synthesis of citrate capped gold nanoparticles using UV induced nucleation. RSC Advances, 2017, 7, 9632-9638.	3.6	36

#	Article	IF	CITATIONS
235	Facile fabrication of durable superhydrophobic SiO <sub>2</sub> /polyurethane composite sponge for continuous separation of oil from water. RSC Advances, 2017, 7, 11362-11366.	3.6	41
236	Superoleophobic surfaces on stainless steel substrates obtained by chemical bath deposition. Micro and Nano Letters, 2017, 12, 76-81.	1.3	19
237	Correlation of Optical Properties, Electronic Structure, and Photocatalytic Activity in Nanostructured Tungsten Oxide. Advanced Materials Interfaces, 2017, 4, 1700064.	3.7	25
238	Chemical Vapor Deposition Synthesis and Optical Properties of Nb <sub>2</sub> O <sub>5</sub> Thin Films with Hybrid Functional Theoretical Insight into the Band Structure and Band Gaps. ACS Applied Materials & Interfaces, 2017, 9, 18031-18038.	8.0	54
239	Photocatalysis: Evidence and Effect of Photogenerated Charge Transfer for Enhanced Photocatalysis in WO <sub>3</sub> /TiO <sub>2</sub> Heterojunction Films: A Computational and Experimental Study (Adv. Funct. Mater. 18/2017). Advanced Functional Materials, 2017, 27, .	14.9	1
240	Interstitial boron-doped anatase TiO <sub>2</sub> thin-films on optical fibres: atmospheric pressure-plasma enhanced chemical vapour deposition as the key for functional oxide coatings on temperature-sensitive substrates. Journal of Materials Chemistry A, 2017, 5, 10836-10842.	10.3	25
241	Buoyancy increase and drag-reduction through a simple superhydrophobic coating. Nanoscale, 2017, 9, 7588-7594.	5.6	141
242	Large-scale fabrication of translucent and repairable superhydrophobic spray coatings with remarkable mechanical, chemical durability and UV resistance. Journal of Materials Chemistry A, 2017, 5, 10622-10631.	10.3	164
243	Enhancing the Magnetic Heating Capacity of Iron Oxide Nanoparticles through Their Postproduction Incorporation into Iron Oxide-Gold Nanocomposites. European Journal of Inorganic Chemistry, 2017, 2017, 2385-2385.	2.0	2
244	Enhanced adsorption capacity of ultralong hydrogen titanate nanobelts for antibiotics. Journal of Materials Chemistry A, 2017, 5, 4352-4358.	10.3	76
245	Water Oxidation Kinetics of Accumulated Holes on the Surface of a TiO <sub>2</sub> Photoanode: A Rate Law Analysis. ACS Catalysis, 2017, 7, 4896-4903.	11.2	105
246	Scaling aerosol assisted chemical vapour deposition: Exploring the relationship between growth rate and film properties. Materials and Design, 2017, 129, 116-124.	7.0	44
247	Electrochemical sensor for discrimination tyrosine enantiomers using graphene quantum dots and β-cyclodextrins composites. Talanta, 2017, 173, 94-100.	5.5	89
248	Optimized Atmospheric-Pressure Chemical Vapor Deposition Thermochromic VO <sub>2</sub> Thin Films for <i>Intelligent</i> Window Applications. ACS Omega, 2017, 2, 1040-1046.	3.5	56
249	Evidence and Effect of Photogenerated Charge Transfer for Enhanced Photocatalysis in WO <sub>3</sub> /TiO <sub>2</sub> Heterojunction Films: A Computational and Experimental Study. Advanced Functional Materials, 2017, 27, 1605413.	14.9	115
250	Dopant stability in multifunctional doped TiO <sub>2</sub> 's under environmental UVA exposure. Environmental Science: Nano, 2017, 4, 1108-1113.	4.3	1
251	Multi-mode application of graphene quantum dots bonded silica stationary phase for high performance liquid chromatography. Journal of Chromatography A, 2017, 1492, 61-69.	3.7	43
252	A free-standing porous silicon-type gel sponge with superhydrophobicity and oleophobicity. RSC Advances, 2017, 7, 31-36.	3.6	12

#	Article	IF	CITATIONS
253	An array of WO <sub>3</sub> and CTO heterojunction semiconducting metal oxide gas sensors used as a tool for explosive detection. Journal of Materials Chemistry A, 2017, 5, 2172-2179.	10.3	50
254	Computational and Experimental Study of Ta <sub>2</sub> O <sub>5</sub> Thin Films. Journal of Physical Chemistry C, 2017, 121, 202-210.	3.1	27
255	A Targeted Functional Design for Highly Efficient and Stable Cathodes for Rechargeable Liâ€lon Batteries. Advanced Functional Materials, 2017, 27, 1604903.	14.9	22
256	Ultrasensitive plano-concave optical microresonators for ultrasound sensing. Nature Photonics, 2017, 11, 714-719.	31.4	255
257	Nanoparticles in explosives detection – the state-of-the-art and future directions. Forensic Science, Medicine, and Pathology, 2017, 13, 490-494.	1.4	14
258	Sensitive and specific detection of explosives in solution and vapour by surface-enhanced Raman spectroscopy on silver nanocubes. Nanoscale, 2017, 9, 16459-16466.	5.6	78
259	Nanoscale, conformal films of graphitic carbon nitride deposited at room temperature: a method for construction of heterojunction devices. Nanoscale, 2017, 9, 16586-16590.	5.6	20
260	Qualitative XANES and XPS Analysis of Substrate Effects in VO <sub>2</sub> Thin Films: A Route to Improving Chemical Vapor Deposition Synthetic Methods?. Journal of Physical Chemistry C, 2017, 121, 20345-20352.	3.1	22
261	Large-Area Fabrication of Droplet Pancake Bouncing Surface and Control of Bouncing State. ACS Nano, 2017, 11, 9259-9267.	14.6	118
262	The <i>in situ</i> synthesis of PbS nanocrystals from lead(II) <i>n</i> -octylxanthate within a 1,3-diisopropenylbenzene–bisphenol A dimethacrylate sulfur copolymer. Royal Society Open Science, 2017, 4, 170383.	2.4	13
263	Table Salt as a Template to Prepare Reusable Porous PVDF–MWCNT Foam for Separation of Immiscible Oils/Organic Solvents and Corrosive Aqueous Solutions. Advanced Functional Materials, 2017, 27, 1702926.	14.9	160
264	Transparent conducting n-type ZnO:Sc – synthesis, optoelectronic properties and theoretical insight. Journal of Materials Chemistry C, 2017, 5, 7585-7597.	5.5	46
265	Plasmonic Gold Nanostars Incorporated into Highâ€Efficiency Perovskite Solar Cells. ChemSusChem, 2017, 10, 3750-3753.	6.8	39
266	Particle size, morphology and phase transitions in hydrothermally produced VO <sub>2</sub> (D). New Journal of Chemistry, 2017, 41, 9216-9222.	2.8	26
267	Phase and morphological control of MoO <sub>3â^'x</sub> nanostructures for efficient cancer theragnosis therapy. Nanoscale, 2017, 9, 11012-11016.	5.6	45
268	Self-standing electrodes with core-shell structures for high-performance supercapacitors. Energy Storage Materials, 2017, 9, 119-125.	18.0	52
269	Switchable changes in the conductance of single-walled carbon nanotube networks on exposure to water vapour. Nanoscale, 2017, 9, 11279-11287.	5.6	6
270	Transparent superhydrophobic PTFE films via one-step aerosol assisted chemical vapor deposition. RSC Advances, 2017, 7, 29275-29283.	3.6	52

#	Article	IF	CITATIONS
271	Superhydrophobic and White Light-Activated Bactericidal Surface through a Simple Coating. ACS Applied Materials & Interfaces, 2017, 9, 29002-29009.	8.0	34
272	Si-doped zinc oxide transparent conducting oxides; nanoparticle optimisation, scale-up and thin film deposition. Journal of Materials Chemistry C, 2017, 5, 8796-8801.	5.5	10
273	Electronic properties of antimony-doped anatase TiO <sub>2</sub> thin films prepared by aerosol assisted chemical vapour deposition. Journal of Materials Chemistry C, 2017, 5, 9694-9701.	5.5	25
274	Through-needle all-optical ultrasound imaging in vivo: a preclinical swine study. Light: Science and Applications, 2017, 6, e17103-e17103.	16.6	90
275	A general method for boosting the supercapacitor performance of graphitic carbon nitride/graphene hybrids. Journal of Materials Chemistry A, 2017, 5, 25545-25554.	10.3	77
276	A Light-Activated Antimicrobial Surface Is Active Against Bacterial, Viral and Fungal Organisms. Scientific Reports, 2017, 7, 15298.	3.3	27
277	Transforming a Simple Commercial Glue into Highly Robust Superhydrophobic Surfaces via Aerosol-Assisted Chemical Vapor Deposition. ACS Applied Materials & Interfaces, 2017, 9, 42327-42335.	8.0	85
278	Super-robust superhydrophobic concrete. Journal of Materials Chemistry A, 2017, 5, 14542-14550.	10.3	170
279	Optical fiber ultrasound transmitter with electrospun carbon nanotube-polymer composite. Applied Physics Letters, 2017, 110, 223701.	3.3	54
280	On the apparent visible-light and enhanced UV-light photocatalytic activity of nitrogen-doped TiO 2 thin films. Journal of Photochemistry and Photobiology A: Chemistry, 2017, 333, 49-55.	3.9	29
281	S, Nâ€Coâ€Doped Grapheneâ€Nickel Cobalt Sulfide Aerogel: Improved Energy Storage and Electrocatalytic Performance. Advanced Science, 2017, 4, 1600214.	11.2	204
282	Nanoparticles Encapsulated in Porous Carbon Matrix Coated on Carbon Fibers: An Ultrastable Cathode for Liâ€lon Batteries. Advanced Energy Materials, 2017, 7, 1601363.	19.5	48
283	{Ni4O4} Cluster Complex to Enhance the Reductive Photocurrent Response on Silicon Nanowire Photocathodes. Nanomaterials, 2017, 7, 33.	4.1	2
284	Optical fiber laser ultrasound transmitter with electrospun composite for minimally invasive medical imaging. , 2017, , .		0
285	Gas Sensing Studies of an n-n Hetero-Junction Array Based on SnO2 and ZnO Composites. Chemosensors, 2016, 4, 3.	3.6	18
286	Nanocellulose Derivative/Silica Hybrid Core-Shell Chiral Stationary Phase: Preparation and Enantioseparation Performance. Molecules, 2016, 21, 561.	3.8	10
287	Aerosol-assisted fabrication of tin-doped indium oxide ceramic thin films from nanoparticle suspensions. Journal of Materials Chemistry C, 2016, 4, 5739-5746.	5.5	8
288	Polyoxometalate Complexes as Precursors to Vanadiumâ€Doped Molybdenum or Tungsten Oxide Thin Films by Means of Aerosolâ€Assisted Chemical Vapour Deposition. ChemPlusChem, 2016, 81, 307-314.	2.8	7

#	Article	IF	CITATIONS
289	Nanocellulose 3, 5â€Dimethylphenylcarbamate Derivative Coated Chiral Stationary Phase: Preparation and Enantioseparation Performance. Chirality, 2016, 28, 376-381.	2.6	27
290	Alâ€; Gaâ€; and Inâ€doped ZnO thin films via aerosol assisted CVD for use as transparent conducting oxides. Physica Status Solidi (A) Applications and Materials Science, 2016, 213, 1346-1352.	1.8	43
291	Thiol-Capped Gold Nanoparticles Swell-Encapsulated into Polyurethane as Powerful Antibacterial Surfaces Under Dark and Light Conditions. Scientific Reports, 2016, 6, 39272.	3.3	54
292	The bactericidal activity of glutaraldehydeâ€impregnated polyurethane. MicrobiologyOpen, 2016, 5, 891-897.	3.0	22
293	Copper-based water repellent and antibacterial coatings by aerosol assisted chemical vapour deposition. Chemical Science, 2016, 7, 5126-5131.	7.4	87
294	Synthesis of Trimeric Organozinc Compounds and their Subsequent Reaction with Oxygen. ChemistryOpen, 2016, 5, 301-305.	1.9	10
295	Enhancing the Antibacterial Activity of Light-Activated Surfaces Containing Crystal Violet and ZnO Nanoparticles: Investigation of Nanoparticle Size, Capping Ligand, and Dopants. ACS Omega, 2016, 1, 334-343.	3.5	41
296	Electrochemical Properties of APCVD αâ€Fe <sub>2</sub> O <sub>3</sub> Nanoparticles at 300 <sup>o</sup> C. ChemistrySelect, 2016, 1, 2228-2234.	1.5	2
297	Controlling the Cross-Sensitivity of Carbon Nanotube-Based Gas Sensors to Water Using Zeolites. ACS Applied Materials & Interfaces, 2016, 8, 28096-28104.	8.0	25
298	Conducting Al and Ga-doped zinc oxides; rapid optimisation and scale-up. Journal of Materials Chemistry A, 2016, 4, 12774-12780.	10.3	14
299	Ethanol sensing characteristics of Zn <sub>0.99</sub> M <sub>0.01</sub> O (M = Al/Ni) nanopowders. Physica Status Solidi (A) Applications and Materials Science, 2016, 213, 203-209.	1.8	5
300	Synthesis of Rutile Nb:TiO <sub>2</sub> Free‣tanding Thin Film at the Liquid–Air Interface. Advanced Materials Interfaces, 2016, 3, 1600361.	3.7	1
301	Power-free water pump based on a superhydrophobic surface: generation of a mushroom-like jet and anti-gravity long-distance transport. Journal of Materials Chemistry A, 2016, 4, 13771-13777.	10.3	16
302	In situ mass spectrometry analysis of chemical vapour deposition of TiO <sub>2</sub> thin films to study gas phase mechanisms. RSC Advances, 2016, 6, 111797-111805.	3.6	6
303	Carbonâ€Nanotube–PDMS Composite Coatings on Optical Fibers for Allâ€Optical Ultrasound Imaging. Advanced Functional Materials, 2016, 26, 8390-8396.	14.9	120
304	Aerosol assisted chemical vapour deposition of transparent conductive aluminum-doped zinc oxide thin films from a zinc triflate precursor. Thin Solid Films, 2016, 616, 477-481.	1.8	9
305	Interstitial Boron-Doped TiO <sub>2</sub> Thin Films: The Significant Effect of Boron on TiO <sub>2</sub> Coatings Grown by Atmospheric Pressure Chemical Vapor Deposition. ACS Applied Materials & Interfaces, 2016, 8, 25024-25029.	8.0	44
306	A single-source precursor approach to solution processed indium arsenide thin films. Journal of Materials Chemistry C, 2016, 4, 6761-6768.	5.5	19

#	Article	IF	CITATIONS
307	Flexible and mechanically robust superhydrophobic silicone surfaces with stable Cassie–Baxter state. Journal of Materials Chemistry A, 2016, 4, 14180-14186.	10.3	71
308	Graphene/nitrogen-doped porous carbon sandwiches for the metal-free oxygen reduction reaction: conductivity versus active sites. Journal of Materials Chemistry A, 2016, 4, 12658-12666.	10.3	99
309	Reactivity of vanadium oxytrichloride with β-diketones and diesters as precursors for vanadium nitride and carbide. Materials and Design, 2016, 108, 780-790.	7.0	15
310	ZnO Rods with Exposed {100} Facets Grown via a Self-Catalyzed Vapor–Solid Mechanism and Their Photocatalytic and Gas Sensing Properties. ACS Applied Materials & Interfaces, 2016, 8, 33335-33342.	8.0	42
311	Fabrication of Long-Term Underwater Superoleophobic Al Surfaces and Application on Underwater Lossless Manipulation of Non-Polar Organic Liquids. Scientific Reports, 2016, 6, 31818.	3.3	18
312	[{VOCl2(CH2(COOEt)2)}4] as a molecular precursor for thermochromic monoclinic VO2 thin films and nanoparticles. Journal of Materials Chemistry C, 2016, 4, 10453-10463.	5.5	6
313	Magnetic hyperthermia controlled drug release in the GI tract: solving the problem of detection. Scientific Reports, 2016, 6, 34271.	3.3	23
314	A SPION-eicosane protective coating for water soluble capsules: Evidence for on-demand drug release triggered by magnetic hyperthermia. Scientific Reports, 2016, 6, 20271.	3.3	19
315	Comparative study of singlet oxygen production by photosensitiser dyes encapsulated in silicone: towards rational design of anti-microbial surfaces. Physical Chemistry Chemical Physics, 2016, 18, 28101-28109.	2.8	31
316	Synthesis and material characterization ofÂamorphous and crystalline (α-) Al <sub>2</sub> O <sub>3</sub> via aerosol assisted chemical vapour deposition. RSC Advances, 2016, 6, 102956-102960.	3.6	27
317	Photo-induced enhanced Raman spectroscopy for universal ultra-trace detection of explosives, pollutants and biomolecules. Nature Communications, 2016, 7, 12189.	12.8	201
318	Plasmonic Nanoprobes for Stimulated Emission Depletion Nanoscopy. ACS Nano, 2016, 10, 10454-10461.	14.6	29
319	Synthesis and characterization of omniphobic surfaces with thermal, mechanical and chemical stability. RSC Advances, 2016, 6, 106491-106499.	3.6	17
320	Scalable Production of Thermochromic Nb-Doped VO <sub>2</sub> Nanomaterials Using Continuous Hydrothermal Flow Synthesis. Journal of Nanoscience and Nanotechnology, 2016, 16, 10104-10111.	0.9	14
321	Zeolite Modified Vanadium Pentoxide Sensors for the Selective Detection of Volatile Organic Compounds. MRS Advances, 2016, 1, 3349-3354.	0.9	6
322	Advanced Compositional Analysis of Nanoparticle-polymer Composites Using Direct Fluorescence Imaging. Journal of Visualized Experiments, 2016, , .	0.3	1
323	Porous carbons from inverse vulcanised polymers. Microporous and Mesoporous Materials, 2016, 232, 189-195.	4.4	34
324	n-Type doped transparent conducting binary oxides: an overview. Journal of Materials Chemistry C, 2016, 4, 6946-6961.	5.5	287

#	Article	IF	CITATIONS
325	Where Do Photogenerated Holes Go in Anatase:Rutile TiO <sub>2</sub> ? A Transient Absorption Spectroscopy Study of Charge Transfer and Lifetime. Journal of Physical Chemistry A, 2016, 120, 715-723.	2.5	128
326	High-Throughput Synthesis, Screening, and Scale-Up of Optimized Conducting Indium Tin Oxides. ACS Combinatorial Science, 2016, 18, 130-137.	3.8	21
327	SWCNT photocathodes sensitised with InP/ZnS core–shell nanocrystals. Journal of Materials Chemistry C, 2016, 4, 3379-3384.	5.5	15
328	Underwater Spontaneous Pumpless Transportation of Nonpolar Organic Liquids on Extreme Wettability Patterns. ACS Applied Materials & Interfaces, 2016, 8, 2942-2949.	8.0	72
329	Superhydrophobic Au/polymer nanocomposite films via AACVD/swell encapsulation tandem synthesis procedure. RSC Advances, 2016, 6, 31146-31152.	3.6	10
330	Designing durable and flexible superhydrophobic coatings and its application in oil purification. Journal of Materials Chemistry A, 2016, 4, 4107-4116.	10.3	94
331	Intelligent Multifunctional VO <sub>2</sub> /SiO <sub>2</sub> /TiO <sub>2</sub> Coatings for Self-Cleaning, Energy-Saving Window Panels. Chemistry of Materials, 2016, 28, 1369-1376.	6.7	221
332	On-demand, magnetic hyperthermia-triggered drug delivery: optimisation for the GI tract. Journal of Materials Chemistry B, 2016, 4, 1704-1711.	5.8	15
333	Graphene quantum dots as additives in capillary electrophoresis for separation cinnamic acid and its derivatives. Analytical Biochemistry, 2016, 500, 38-44.	2.4	25
334	White light-activated antimicrobial surfaces: effect of nanoparticles type on activity. Journal of Materials Chemistry B, 2016, 4, 2199-2207.	5.8	19
335	Bismuth oxyhalides: synthesis, structure and photoelectrochemical activity. Chemical Science, 2016, 7, 4832-4841.	7.4	252
336	Antibacterial properties of Cu–ZrO2thin films prepared via aerosol assisted chemical vapour deposition. Journal of Materials Chemistry B, 2016, 4, 666-671.	5.8	12
337	Photo-activity and low resistivity in N/Nb Co-doped TiO <sub>2</sub> thin films by combinatorial AACVD. Journal of Materials Chemistry A, 2016, 4, 407-415.	10.3	18
338	Multichannel Detection and Differentiation of Explosives with a Quantum Dot Array. ACS Nano, 2016, 10, 1139-1146.	14.6	120
339	White Light-Activated Antimicrobial Paint using Crystal Violet. ACS Applied Materials & Interfaces, 2016, 8, 15033-15039.	8.0	25
340	Synthesis of superhydrophobic polymer/tungsten (VI) oxide nanocomposite thin films. European Journal of Chemistry, 2016, 7, 139-145.	0.6	5
341	Oil Spills: Barrel-Shaped Oil Skimmer Designed for Collection of Oil from Spills (Adv. Mater.) Tj ETQq1 1 0.78431	4 rgBT /O	verlock 10 Tf
342	Doping Group IIB Metal Ions into Quantum Dot Shells via the Oneâ€Pot Decomposition of Metalâ€Dithiocarbamates. Advanced Optical Materials, 2015, 3, 704-712.	7.3	19

#	Article	IF	CITATIONS
343	Aerosolâ€Assisted Chemicalâ€Vapour Deposition of Zinc Oxide from Singleâ€&ource βâ€Iminoesterate Precursors. European Journal of Inorganic Chemistry, 2015, 2015, 3658-3665.	2.0	17
344	Barrelâ€6haped Oil Skimmer Designed for Collection of Oil from Spills. Advanced Materials Interfaces, 2015, 2, 1500350.	3.7	112
345	Synthesis and Characterisation of Various Diester and Triester Adducts of TiCl <sub>4</sub> . European Journal of Inorganic Chemistry, 2015, 2015, 3666-3673.	2.0	2
346	Magnesium Oxide Thin Films with Tunable Crystallographic Preferred Orientation via Aerosolâ€Assisted CVD. Chemical Vapor Deposition, 2015, 21, 145-149.	1.3	4
347	A Hierarchical MoO <sub>2</sub> /Au/MnO <sub>2</sub> HeteroÂstructure with Enhanced Electrochemical Performance for Application as Supercapacitor. European Journal of Inorganic Chemistry, 2015, 2015, 3764-3768.	2.0	10
348	Nanoparticle–sulphur "inverse vulcanisation―polymer composites. Chemical Communications, 2015, 51, 10467-10470.	4.1	35
349	Suspension plasma sprayed coatings using dilute hydrothermally produced titania feedstocks for photocatalytic applications. Journal of Materials Chemistry A, 2015, 3, 12680-12689.	10.3	21
350	Advanced analysis of nanoparticle composites $\hat{a} \in \hat{a}$ a means toward increasing the efficiency of functional materials. RSC Advances, 2015, 5, 53789-53795.	3.6	16
351	Fabrication of optimized oil–water separation devices through the targeted treatment of silica meshes. Science and Technology of Advanced Materials, 2015, 16, 055006.	6.1	16
352	Enhanced Bactericidal Activity of Silver Thin Films Deposited via Aerosol-Assisted Chemical Vapor Deposition. ACS Applied Materials & Interfaces, 2015, 7, 28616-28623.	8.0	18
353	The use of zinc oxide nanoparticles to enhance the antibacterial properties of light-activated polydimethylsiloxane containing crystal violet. RSC Advances, 2015, 5, 8806-8813.	3.6	32
354	The vapour phase detection of explosive markers and derivatives using two fluorescent metal–organic frameworks. Journal of Materials Chemistry A, 2015, 3, 6351-6359.	10.3	69
355	Spherical β-cyclodextrin-silica hybrid materials for multifunctional chiral stationary phases. Journal of Chromatography A, 2015, 1383, 70-78.	3.7	31
356	Dualâ€Mechanism Antimicrobial Polymer–ZnO Nanoparticle and Crystal Violetâ€Encapsulated Silicone. Advanced Functional Materials, 2015, 25, 1367-1373.	14.9	94
357	A Method for Synthesis of Renewable Cu <sub>2</sub> O Junction Composite Electrodes and Their Photoelectrochemical Properties. ACS Sustainable Chemistry and Engineering, 2015, 3, 710-717.	6.7	50
358	One pot synthesis of nickel foam supported self-assembly of NiWO <sub>4</sub> and CoWO <sub>4</sub> nanostructures that act as high performance electrochemical capacitor electrodes. Journal of Materials Chemistry A, 2015, 3, 14272-14278.	10.3	167
359	Aerosol assisted chemical vapour deposition of a ZrO <sub>2</sub> –TiO <sub>2</sub> composite thin film with enhanced photocatalytic activity. RSC Advances, 2015, 5, 67944-67950.	3.6	19
360	Tungsten Doped TiO2 with Enhanced Photocatalytic and Optoelectrical Properties via Aerosol Assisted Chemical Vapor Deposition. Scientific Reports, 2015, 5, 10952.	3.3	122

#	Article	IF	CITATIONS
361	Lethal photosensitisation of Staphylococcus aureus and Escherichia coli using crystal violet and zinc oxide-encapsulated polyurethane. Journal of Materials Chemistry B, 2015, 3, 6490-6500.	5.8	43
362	High-throughput synthesis of core–shell and multi-shelled materials by fluidised bed chemical vapour deposition. Case study: double-shell rutile–anatase particles. Journal of Materials Chemistry A, 2015, 3, 17241-17247.	10.3	6
363	Photosensitisation studies of silicone polymer doped with methylene blue and nanogold for antimicrobial applications. RSC Advances, 2015, 5, 54830-54842.	3.6	28
364	Silicalite-1/glass fibre substrates for enhancing the photocatalytic activity of TiO2. RSC Advances, 2015, 5, 6970-6975.	3.6	3
365	Multifunctional P-Doped TiO <sub>2</sub> Films: A New Approach to Self-Cleaning, Transparent Conducting Oxide Materials. Chemistry of Materials, 2015, 27, 3234-3242.	6.7	113
366	Hydrophilic patterning of superhydrophobic surfaces by atmosphericâ€pressure plasma jet. Micro and Nano Letters, 2015, 10, 105-108.	1.3	35
367	Incorporation of crystal violet, methylene blue and safranin O into a copolymer emulsion; the development of a novel antimicrobial paint. RSC Advances, 2015, 5, 26364-26375.	3.6	17
368	CuInS <sub>2</sub> /ZnS nanocrystals as sensitisers for NiO photocathodes. Journal of Materials Chemistry A, 2015, 3, 13324-13331.	10.3	35
369	Transient Absorption Spectroscopy of Anatase and Rutile: The Impact of Morphology and Phase on Photocatalytic Activity. Journal of Physical Chemistry C, 2015, 119, 10439-10447.	3.1	135
370	Functional thin film coatings incorporating gold nanoparticles in a transparent conducting fluorine doped tin oxide matrix. Journal of Materials Chemistry C, 2015, 3, 1118-1125.	5.5	19
371	Antimicrobial Surfaces: Dualâ€Mechanism Antimicrobial Polymer–ZnO Nanoparticle and Crystal Violetâ€Encapsulated Silicone (Adv. Funct. Mater. 9/2015). Advanced Functional Materials, 2015, 25, 1366-1366.	14.9	4
372	Origin of High Mobility in Molybdenum-Doped Indium Oxide. Chemistry of Materials, 2015, 27, 2788-2796.	6.7	71
373	Robust self-cleaning surfaces that function when exposed to either air or oil. Science, 2015, 347, 1132-1135.	12.6	1,494
374	Environmental sensing semiconducting nanoceramics made using a continuous hydrothermal synthesis pilot plant. Sensors and Actuators B: Chemical, 2015, 217, 136-145.	7.8	13
375	Potent Antibacterial Activity of Copper Embedded into Silicone and Polyurethane. ACS Applied Materials & Interfaces, 2015, 7, 22807-22813.	8.0	71
376	Creating robust superamphiphobic coatings for both hard and soft materials. Journal of Materials Chemistry A, 2015, 3, 20999-21008.	10.3	123
377	Urchin-like MnO2 capped ZnO nanorods as high-rate and high-stability pseudocapacitor electrodes. Electrochimica Acta, 2015, 186, 1-6.	5.2	24
378	Self-propagating high-temperature synthesis of aluminum substituted lanthanum ferrites LaFe <sub>1â^'x</sub> Al <sub>x</sub> O <sub>3</sub> (0 ≤ ≤.0). New Journal of Chemistry, 2015, 39, 9834-9840.	2.8	8

#	Article	IF	CITATIONS
379	Synthesis and characterisation of novel aluminium and gallium precursors for chemical vapour deposition. New Journal of Chemistry, 2015, 39, 6585-6592.	2.8	22
380	Highly Photocatalytically Active Iron(III) Titanium Oxide Thin films via Aerosolâ€Assisted CVD. Chemical Vapor Deposition, 2015, 21, 21-25.	1.3	8
381	Enhanced gas sensing performance of indium doped zinc oxide nanopowders. RSC Advances, 2015, 5, 85767-85774.	3.6	15
382	Direct and continuous synthesis of VO <sub>2</sub> nanoparticles. Nanoscale, 2015, 7, 18686-18693.	5.6	47
383	Influencing FTO thin film growth with thin seeding layers: a route to microstructural modification. Journal of Materials Chemistry C, 2015, 3, 9359-9368.	5.5	34
384	The use of time resolved aerosol assisted chemical vapour deposition in mapping metal oxide thin film growth and fine tuning functional properties. Journal of Materials Chemistry A, 2015, 3, 4811-4819.	10.3	5
385	A gas-sensing array produced from screen-printed, zeolite-modified chromium titanate. Measurement Science and Technology, 2015, 26, 085102.	2.6	10
386	On the nature of niobium substitution in niobium doped titania thin films by AACVD and its impact on electrical and optical properties. Journal of Materials Chemistry A, 2015, 3, 17755-17762.	10.3	29
387	Scalable route to CH <sub>3</sub> NH <sub>3</sub> PbI <sub>3</sub> perovskite thin films by aerosol assisted chemical vapour deposition. Journal of Materials Chemistry A, 2015, 3, 9071-9073.	10.3	75
388	TiO <sub>2</sub> oated CoCrMo: Improving the osteogenic differentiation and adhesion of mesenchymal stem cells <i>in vitro</i> . Journal of Biomedical Materials Research - Part A, 2015, 103, 1208-1217.	4.0	24
389	Effect of pretreatment temperature on the photocatalytic activity of microwave irradiated porous nanocrystalline ZnO. New Journal of Chemistry, 2015, 39, 321-332.	2.8	29
390	Light-activated antibacterial screen protectors for mobile telephones and tablet computers. Journal of Photochemistry and Photobiology A: Chemistry, 2015, 296, 19-24.	3.9	21
391	Ferrite Materials Produced From Self-Propagating High-Temperature Synthesis for Gas Sensing Applications. IEEE Sensors Journal, 2015, 15, 196-200.	4.7	8
392	Superhydrophobic silica wool—a facile route to separating oil and hydrophobic solvents from water. Science and Technology of Advanced Materials, 2014, 15, 065003.	6.1	13
393	Functionalised gold and titania nanoparticles and surfaces for use as antimicrobial coatings. Faraday Discussions, 2014, 175, 273-287.	3.2	16
394	Laser-generated ultrasound with optical fibres using functionalised carbon nanotube composite coatings. Applied Physics Letters, 2014, 104, .	3.3	101
395	Combinatorial Atmospheric Pressure Chemical Vapor Deposition of F:TiO <sub>2</sub> ; the Relationship between Photocatalysis and Transparent Conducting Oxide Properties. Advanced Functional Materials, 2014, 24, 1758-1771.	14.9	44
396	Synthesis and Structural Characterization of βâ€Ketoiminate‣tabilized Gallium Hydrides for Chemical Vapor Deposition Applications. Chemistry - A European Journal, 2014, 20, 10503-10513.	3.3	9

#	Article	IF	CITATIONS
397	Visible Light Photocatalytic Activity in AACVDâ€Prepared Nâ€modified TiO <sub>2</sub> Thin Films. Chemical Vapor Deposition, 2014, 20, 91-97.	1.3	14
398	Photocatalytic Evidence of the Rutileâ€ŧoâ€Anatase Electron Transfer in Titania. Advanced Materials Interfaces, 2014, 1, 1400069.	3.7	43
399	Aerosolâ€Assisted Chemical Vapour Deposition of Transparent Zinc Gallate Films. ChemPlusChem, 2014, 79, 1024-1029.	2.8	11
400	Mesenchymal stem cell response to UV-photofunctionalized TiO <sub>2</sub> coated CoCrMo. RSC Advances, 2014, 4, 59847-59857.	3.6	3
401	N-doped TiO2 visible light photocatalyst films via a sol–gel route using TMEDA as the nitrogen source. Journal of Photochemistry and Photobiology A: Chemistry, 2014, 281, 27-34.	3.9	37
402	Light-activated antimicrobial surfaces with enhanced efficacy induced by a dark-activated mechanism. Chemical Science, 2014, 5, 2216-2223.	7.4	52
403	The interaction of gold and silver nanoparticles with a range of anionic and cationic dyes. Physical Chemistry Chemical Physics, 2014, 16, 6050-6059.	2.8	37
404	Solution Processing Route to Multifunctional Titania Thin Films: Highly Conductive and Photcatalytically Active Nb:TiO <sub>2</sub> . Advanced Functional Materials, 2014, 24, 5075-5085.	14.9	93
405	A fast and effective method for N-doping TiO2 by post treatment with liquid ammonia: visible light photocatalysis. Thin Solid Films, 2014, 562, 223-228.	1.8	20
406	PbO-Modified TiO <sub>2</sub> Thin Films: A Route to Visible Light Photocatalysts. Langmuir, 2014, 30, 624-630.	3.5	50
407	Critical influence of surface nitrogen species on the activity of N-doped TiO2 thin-films during photodegradation of stearic acid under UV light irradiation. Applied Catalysis B: Environmental, 2014, 160-161, 582-588.	20.2	44
408	Combinatorial Atmospheric Pressure CVD of a Composite TiO <sub>2</sub> /SnO <sub>2</sub> Thin Film. Chemical Vapor Deposition, 2014, 20, 69-79.	1.3	12
409	Aerosolâ€Assisted Chemical Vapour Deposition of a Copper Gallium Oxide Spinel. ChemPlusChem, 2014, 79, 122-127.	2.8	21
410	Temperature and thickness-dependent growth behaviour and opto-electronic properties of Ga-doped ZnO films prepared by aerosol-assisted chemical vapour deposition. Journal of Materials Chemistry A, 2014, 2, 17174-17182.	10.3	28
411	Prolonging the circulatory retention of SPIONs using dextran sulfate: in vivo tracking achieved by functionalisation with near-infrared dyes. Faraday Discussions, 2014, 175, 41-58.	3.2	20
412	Aerosol-assisted deposition of gold nanoparticle-tin dioxide composite films. RSC Advances, 2014, 4, 13182-13190.	3.6	15
413	The gas sensing properties of zeolite modified zinc oxide. Journal of Materials Chemistry A, 2014, 2, 4758-4764.	10.3	43
414	Single-step synthesis of doped TiO2 stratified thin-films by atmospheric-pressure chemical vapour deposition. Journal of Materials Chemistry A, 2014, 2, 7082.	10.3	7

#	Article	IF	CITATIONS
415	Lithiated MoO <sub>2</sub> Nanorods with Greatly Improved Electrochemical Performance for Lithium Ion Batteries. European Journal of Inorganic Chemistry, 2014, 2014, 352-356.	2.0	13
416	Polydimethylsiloxane coated glass frits for low-cost and reusable water–organic solvent separation. Chemical Communications, 2014, 50, 12656-12658.	4.1	12
417	Single-walled carbon nanotube composite inks for printed gas sensors: enhanced detection of NO <sub>2</sub> , NH <sub>3</sub> , EtOH and acetone. RSC Advances, 2014, 4, 51395-51403.	3.6	40
418	Water droplets bouncing on superhydrophobic soft porous materials. Journal of Materials Chemistry A, 2014, 2, 12177-12184.	10.3	45
419	Creating superhydrophobic mild steel surfaces for water proofing and oil–water separation. Journal of Materials Chemistry A, 2014, 2, 11628-11634.	10.3	153
420	The antibacterial properties of light-activated polydimethylsiloxane containing crystal violet. RSC Advances, 2014, 4, 51711-51715.	3.6	21
421	Transparent conductive aluminium and fluorine co-doped zinc oxide films via aerosol assisted chemical vapour deposition. RSC Advances, 2014, 4, 49723-49728.	3.6	42
422	Copperâ€Đoped CdSe/ZnS Quantum Dots: Controllable Photoactivated Copper(I) Cation Storage and Release Vectors for Catalysis. Angewandte Chemie - International Edition, 2014, 53, 1598-1601.	13.8	58
423	Assessing the potential of metal oxide semiconducting gas sensors for illicit drug detection markers. Journal of Materials Chemistry A, 2014, 2, 8952-8960.	10.3	35
424	Aerosol assisted chemical vapor deposition of conductive and photocatalytically active tantalum doped titanium dioxide films. Journal of Materials Chemistry A, 2014, 2, 12849.	10.3	42
425	A simple and low-cost method for the preparation of self-supported TiO <sub>2</sub> –WO <sub>3</sub> ceramic heterojunction wafers. Journal of Materials Chemistry A, 2014, 2, 17602-17608.	10.3	19
426	Self-Driven One-Step Oil Removal from Oil Spill on Water via Selective-Wettability Steel Mesh. ACS Applied Materials & Interfaces, 2014, 6, 19858-19865.	8.0	226
427	Silver enhanced TiO <sub>2</sub> thin films: photocatalytic characterization using aqueous solutions of tris(hydroxymethyl)aminomethane. Dalton Transactions, 2014, 43, 344-351.	3.3	17
428	Combinatorial aerosol assisted chemical vapour deposition of a photocatalytic mixed SnO <sub>2</sub> /TiO <sub>2</sub> thin film. Journal of Materials Chemistry A, 2014, 2, 5108-5116.	10.3	32
429	Antimicrobial activity of copper and copper( <scp>i</scp> ) oxide thin films deposited via aerosol-assisted CVD. Journal of Materials Chemistry B, 2014, 2, 2855-2860.	5.8	73
430	Electrochemical fabrication of superhydrophobic Zn surfaces. Applied Surface Science, 2014, 315, 346-352.	6.1	42
431	A low cost synthesis method for functionalised iron oxide nanoparticles for magnetic hyperthermia from readily available materials. Faraday Discussions, 2014, 175, 83-95.	3.2	12
432	Organic–inorganic hybrid materials: nanoparticle containing organogels with myriad applications. Chemical Communications, 2014, 50, 14418-14420.	4.1	28

#	Article	IF	CITATIONS
433	A novel damage-tolerant superhydrophobic and superoleophilic material. Journal of Materials Chemistry A, 2014, 2, 9002-9006.	10.3	65
434	Investigation of a Branchlike MoO <sub>3</sub> /Polypyrrole Hybrid with Enhanced Electrochemical Performance Used as an Electrode in Supercapacitors. ACS Applied Materials & Interfaces, 2014, 6, 1125-1130.	8.0	167
435	Gas Sensing Studies of a n-n Hetero-Junction Array Based on WO <sub>3</sub> and ZnO Composites. IEEE Sensors Journal, 2014, 14, 3137-3147.	4.7	22
436	The Gas Sensing Properties of Zinc Stannates Prepared by Self-Propagating High-Temperature Synthesis. Sensor Letters, 2014, 12, 1567-1571.	0.4	1
437	Band alignment of rutile and anatase TiO2. Nature Materials, 2013, 12, 798-801.	27.5	1,924
438	Highly Sensitive ZnO Nanorod- and Nanoprism-Based NO <sub>2</sub> Gas Sensors: Size and Shape Control Using a Continuous Hydrothermal Pilot Plant. Langmuir, 2013, 29, 10603-10609.	3.5	89
439	Nanostructured tungsten oxide gas sensors prepared by electric field assisted aerosol assisted chemical vapour deposition. Journal of Materials Chemistry A, 2013, 1, 1827-1833.	10.3	43
440	Atmospheric pressure chemical vapour deposition of vanadium arsenide thin films via the reaction of VCl4 or VOCl3 with tBuAsH2. Thin Solid Films, 2013, 537, 171-175.	1.8	2
441	Enhanced transparent-conducting fluorine-doped tin oxide films formed by Aerosol-Assisted Chemical Vapour Deposition. Journal of Materials Chemistry C, 2013, 1, 984-996.	5.5	100
442	An EXAFS study on the photo-assisted growth of silver nanoparticles on titanium dioxide thin-films and the identification of their photochromic states. Physical Chemistry Chemical Physics, 2013, 15, 8254.	2.8	16
443	Self-cleaning superhydrophobic surface based on titanium dioxide nanowires combined with polydimethylsiloxane. Applied Surface Science, 2013, 284, 319-323.	6.1	125
444	Facile fabrication of stable superhydrophobic SiO2/polystyrene coating and separation of liquids with different surface tension. Chemical Engineering Journal, 2013, 231, 414-419.	12.7	88
445	Rapid synthesis of gold nanostructures with cyclic and linear ketones. RSC Advances, 2013, 3, 21919.	3.6	14
446	Thermal relaxation and collective dynamics of interacting aerosol-generated hexagonal NiFe2O4 nanoparticles. Physical Chemistry Chemical Physics, 2013, 15, 20830.	2.8	10
447	CVD and precursor chemistry of transition metal nitrides. Coordination Chemistry Reviews, 2013, 257, 2073-2119.	18.8	102
448	TiO2-based transparent conducting oxides; the search for optimum electrical conductivity using a combinatorial approach. Journal of Materials Chemistry C, 2013, 1, 6335.	5.5	32
449	Photobactericidal polymers; the incorporation of crystal violet and nanogold into medical grade silicone. RSC Advances, 2013, 3, 18383.	3.6	42
450	The room temperature formation of gold nanoparticles from the reaction of cyclohexanone and auric acid; a transition from dendritic particles to compact shapes and nanoplates. Journal of Materials Chemistry A, 2013, 1, 7351.	10.3	30

#	Article	IF	CITATIONS
451	Atmospheric pressure chemical vapour deposition of boron doped titanium dioxide for photocatalytic water reduction and oxidation. Physical Chemistry Chemical Physics, 2013, 15, 16788.	2.8	31
452	Relationship between surface hydrophobicity and water bounces – a dynamic method for accessing surface hydrophobicity. Journal of Materials Chemistry A, 2013, 1, 799-804.	10.3	19
453	Zeolite films: a new synthetic approach. Journal of Materials Chemistry A, 2013, 1, 1388-1393.	10.3	5
454	Titania Coated Mica via Chemical Vapour Deposition, Post N-doped by Liquid Ammonia Treatment. Physics Procedia, 2013, 46, 111-117.	1.2	3
455	Shining light on materials — A self-sterilising revolution. Advanced Drug Delivery Reviews, 2013, 65, 570-580.	13.7	83
456	Halide doping effects on transparent conducting oxides formed by aerosol assisted chemical vapour deposition. Thin Solid Films, 2013, 532, 26-30.	1.8	17
457	A general method for the incorporation of nanoparticles into superhydrophobic films by aerosol assisted chemical vapour deposition. Journal of Materials Chemistry A, 2013, 1, 4336.	10.3	47
458	Air purification by heterogeneous photocatalytic oxidation with multi-doped thin film titanium dioxide. Thin Solid Films, 2013, 537, 131-136.	1.8	15
459	Mesoporous silica-supported copper-catalysts for homocoupling reaction of terminal alkynes at room-temperature. New Journal of Chemistry, 2013, 37, 1343.	2.8	37
460	Self-assembly of metallic nanoparticles into one dimensional arrays. Journal of Materials Chemistry A, 2013, 1, 6985.	10.3	54
461	Combinatorial Atmospheric Pressure Chemical Vapor Deposition of Graded TiO <sub>2</sub> –VO <sub>2</sub> Mixed-Phase Composites and Their Dual Functional Property as Self-Cleaning and Photochromic Window Coatings. ACS Combinatorial Science, 2013, 15, 309-319.	3.8	53
462	Aerosol-assisted delivery of precursors for chemical vapour deposition: expanding the scope of CVD for materials fabrication. Dalton Transactions, 2013, 42, 9406.	3.3	224
463	Calcium phosphate-based materials of natural origin showing photocatalytic activity. Journal of Materials Chemistry A, 2013, 1, 6452.	10.3	57
464	Superhydrophobic Surfaces as an On-Chip Microfluidic Toolkit for Total Droplet Control. Analytical Chemistry, 2013, 85, 5405-5410.	6.5	38
465	Aerosol assisted chemical vapour deposition of hydrophobic TiO2–SnO2 composite film with novel microstructure and enhanced photocatalytic activity. Journal of Materials Chemistry A, 2013, 1, 6271.	10.3	55
466	A bioinspired solution for spectrally selective thermochromic VO_2 coated intelligent glazing. Optics Express, 2013, 21, A750.	3.4	90
467	Superhydrophobic polymer-coated copper-mesh; membranes for highly efficient oil–water separation. Journal of Materials Chemistry A, 2013, 1, 5943.	10.3	306

468 Ferrite materials for gas sensing applications. , 2013, , .

#	Article	IF	CITATIONS
469	Gas sensing studies of an n-n heterojunction metal oxide semiconductor sensor array based on WO <inf>3</inf> and ZnO composites. , 2013, , .		5
470	Chromatographic Evaluation of Octadecyl-Bonded SiO2/SiO2-Based Stationary Phase for Reversed-Phase High Performance Liquid Chromatography. Journal of Inorganic and Organometallic Polymers and Materials, 2013, 23, 1445-1450.	3.7	5
471	Detection of explosive markers using zeolite modified gas sensors. Journal of Materials Chemistry A, 2013, 1, 2613.	10.3	36
472	Improved Texturing and Photocatalytic Efficiency in Ti <scp>O</scp> <sub>2</sub> Films Grown Using Aerosolâ€ <scp>A</scp> ssisted <scp>CVD</scp> and Atmospheric Pressure CVD. Chemical Vapor Deposition, 2013, 19, 355-362.	1.3	6
473	A novel bone cement impregnated with silver–tiopronin nanoparticles: its antimicrobial, cytotoxic, and mechanical properties. International Journal of Nanomedicine, 2013, 8, 2227.	6.7	62
474	Control of ZnO Nanostructures via Vapor Transport. Chemical Vapor Deposition, 2012, 18, 282-288.	1.3	2
475	Incorporation of methylene blue and nanogold into polyvinyl chloride catheters; a new approach for light-activated disinfection of surfaces. Journal of Materials Chemistry, 2012, 22, 15388.	6.7	62
476	Tantalum and Titanium doped In <sub>2</sub> O <sub>3</sub> Thin Films by Aerosol-Assisted Chemical Vapor Deposition and their Gas Sensing Properties. Chemistry of Materials, 2012, 24, 2864-2871.	6.7	61
477	Facile approach for preparation of stable water-repellent nanoparticle coating. Applied Surface Science, 2012, 258, 7907-7911.	6.1	15
478	Photocatalytic activity of needle-like TiO2/WO3â^'x thin films prepared by chemical vapour deposition. Journal of Photochemistry and Photobiology A: Chemistry, 2012, 239, 60-64.	3.9	34
479	Does a Photocatalytic Synergy in an Anatase–Rutile TiO <sub>2</sub> Composite Thinâ€Film Exist?. Chemistry - A European Journal, 2012, 18, 13048-13058.	3.3	45
480	Aerosol Assisted Chemical Vapor Deposition of Transparent Conductive Zinc Oxide Films. Chemistry of Materials, 2012, 24, 4704-4710.	6.7	78
481	Inorganic thin-film combinatorial studies for rapidly optimising functional properties. Chemical Society Reviews, 2012, 41, 738-781.	38.1	44
482	Gas Sensing with Nano-Indium Oxides (In <sub>2</sub> O <sub>3</sub> ) Prepared via Continuous Hydrothermal Flow Synthesis. Langmuir, 2012, 28, 1879-1885.	3.5	160
483	Group 13 β-Ketoiminate Compounds: Gallium Hydride Derivatives As Molecular Precursors to Thin Films of Ga2O3. Inorganic Chemistry, 2012, 51, 6385-6395.	4.0	33
484	Electric field-assisted levitation-jet aerosol synthesis of Ni/NiO nanoparticles. Journal of Materials Chemistry, 2012, 22, 11214.	6.7	41
485	The gas sensing properties of some complex metal oxides prepared by self-propagating high-temperature synthesis. Materials Letters, 2012, 75, 36-38.	2.6	29
486	Superhydrophobic Photocatalytic Surfaces through Direct Incorporation of Titania Nanoparticles into a Polymer Matrix by Aerosol Assisted Chemical Vapor Deposition. Advanced Materials, 2012, 24, 3505-3508.	21.0	167

#	Article	IF	CITATIONS
487	Selfâ€Assembled Ultraâ€High Aspect Ratio Silver Nanochains. Advanced Materials, 2012, 24, 5227-5235.	21.0	16
488	Gallium Hydride Complexes Stabilised by Multidentate Alkoxide Ligands: Precursors to Thin Films of Ga <sub>2</sub> O <sub>3</sub> at Low Temperatures. Chemistry - A European Journal, 2012, 18, 6079-6087.	3.3	20
489	The Effect of Solvent on the Phase of Titanium Dioxide Deposited by Aerosolâ€assisted CVD. Chemical Vapor Deposition, 2012, 18, 126-132.	1.3	30
490	Production of Predominantly Anatase Thin Films on Various Grades of Steel and Other Metallic Substrates From TiCl <sub>4</sub> and Ethyl Acetate by Atmospheric Pressure CVD. Chemical Vapor Deposition, 2012, 18, 133-139.	1.3	15
491	CVD Production of Doped Titanium Dioxide Thin Films. Chemical Vapor Deposition, 2012, 18, 89-101.	1.3	35
492	Special Section on the CVD of TiO2 and Doped TiO2 Films. Chemical Vapor Deposition, 2012, 18, 87-88.	1.3	4
493	Mechanochemistry: opportunities for new and cleaner synthesis. Chemical Society Reviews, 2012, 41, 413-447.	38.1	2,281
494	A neutron diffraction study of oxygen and nitrogen ordering in a kinetically stable orthorhombic iron doped titanium oxynitride. Journal of Solid State Chemistry, 2012, 190, 169-173.	2.9	2
495	Silver loaded WO3â^'x/TiO2 composite multifunctional thin films. Thin Solid Films, 2012, 520, 5516-5520.	1.8	15
496	Titanium arsenide films from the atmospheric pressure chemical vapour deposition of tetrakisdimethylamidotitanium and tert-butylarsine. Dalton Transactions, 2011, 40, 10664.	3.3	10
497	Superhydrophobic silica films on glass formed by hydrolysis of an acidic aerosol of tetraethylorthosilicate. Journal of Materials Chemistry, 2011, 21, 9362.	6.7	25
498	The use of combinatorial aerosol-assisted chemical vapour deposition for the formation of gallium-indium-oxide thin films. Journal of Materials Chemistry, 2011, 21, 12644.	6.7	22
499	An investigation into the effect of thickness of titanium dioxide and gold–silver nanoparticle titanium dioxide composite thin-films on photocatalytic activity and photo-induced oxygen production in a sacrificial system. Journal of Materials Chemistry, 2011, 21, 6854.	6.7	31
500	The relationship between photocatalytic activity and photochromic state of nanoparticulate silver surface loaded titanium dioxide thin-films. Physical Chemistry Chemical Physics, 2011, 13, 13827.	2.8	36
501	Oxide Nanoparticle Thin Films Created Using Molecular Templates. Journal of Physical Chemistry C, 2011, 115, 13151-13157.	3.1	1
502	Aerosol-Assisted Chemical Vapor Deposition of Transparent Conductive Galliumâ^'Indiumâ^'Oxide Films. Chemistry of Materials, 2011, 23, 1719-1726.	6.7	59
503	Discrimination Effects in Zeolite Modified Metal Oxide Semiconductor Gas Sensors. IEEE Sensors Journal, 2011, 11, 1145-1151.	4.7	34
504	Efficacy of a Novel Light-Activated Antimicrobial Coating for Disinfecting Hospital Surfaces. Infection Control and Hospital Epidemiology, 2011, 32, 1130-1132.	1.8	27

#	Article	IF	CITATIONS
505	CVD of copper and copper oxide thin films via the in situ reduction of copper(ii) nitrate—a route to conformal superhydrophobic coatings. Journal of Materials Chemistry, 2011, 21, 14712.	6.7	48
506	Nitrogen-doped TiO <sub>2</sub> thin films: photocatalytic applications for healthcare environments. Dalton Transactions, 2011, 40, 1635-1640.	3.3	153
507	Nanoparticles: their potential use in antibacterial photodynamic therapy. Photochemical and Photobiological Sciences, 2011, 10, 712-720.	2.9	173
508	Antimicrobial Properties of Light-activated Polyurethane Containing Indocyanine Green. Journal of Biomaterials Applications, 2011, 25, 387-400.	2.4	25
509	Combinatorial Atmospheric Pressure Chemical Vapor Deposition (cAPCVD): A Route to Functional Property Optimization. Journal of the American Chemical Society, 2011, 133, 20458-20467.	13.7	54
510	Synthetic and Structural Studies of Donor-Functionalized Alkoxy Derivatives of Gallium. Inorganic Chemistry, 2011, 50, 9491-9498.	4.0	20
511	Water droplet bouncing—a definition for superhydrophobic surfaces. Chemical Communications, 2011, 47, 12059.	4.1	125
512	Lethal photosensitisation of bacteria using a tin chlorin e6–glutathione–gold nanoparticle conjugate. Journal of Materials Chemistry, 2011, 21, 4189.	6.7	31
513	Zeolite-modified WO3 gas sensors – Enhanced detection of NO2. Sensors and Actuators B: Chemical, 2011, 160, 475-482.	7.8	52
514	Antimicrobial activity of polyurethane embedded with methylene blue, toluidene blue and gold nanoparticles against Staphylococcus aureus; illuminated with white light. Materials Chemistry and Physics, 2011, 129, 446-450.	4.0	65
515	Visible light photocatalysts—N-doped TiO2 by sol–gel, enhanced with surface bound silver nanoparticle islands. Journal of Materials Chemistry, 2011, 21, 11854.	6.7	56
516	SHS of metal-oxide systems in a DC magnetic field: Part 1. TRXRD and thermal imaging studies of the Fe-Fe2O3 system. International Journal of Self-Propagating High-Temperature Synthesis, 2011, 20, 40-47.	0.5	0
517	SHS of transition metal-oxide systems in a DC magnetic field: Part 2. TRXRD, thermal imaging, and chemomagnetic studies of metal-oxide systems. International Journal of Self-Propagating High-Temperature Synthesis, 2011, 20, 48-52.	0.5	0
518	Study of the adhesion of Staphylococcus aureus to coated glass substrates. Journal of Materials Science, 2011, 46, 6355-6363.	3.7	20
519	Novel ion pairs obtained from the reaction of titanium(IV) halides with simple arsane ligands. Acta Crystallographica Section C: Crystal Structure Communications, 2011, 67, m96-m99.	0.4	5
520	Di-μ-chlorido-bis[dichloridobis(methylamido-κN)bis(methylamine-κN)titanium(IV)]. Acta Crystallographica Section C: Crystal Structure Communications, 2011, 67, m234-m236.	0.4	1
521	Gallium and Indium βâ€Diketonate Complexes: AACVD of [In(thd) <sub>3</sub> ] and the Attempted Synthesis of Gallium and Indium Bis(βâ€diketonates). European Journal of Inorganic Chemistry, 2011, 2011, 1953-1960.	2.0	24
522	Oneâ€Pot Synthesis of Coreâ€Shell Silverâ€Gold Nanoparticle Solutions and Their Interaction with Methylene Blue Dye. European Journal of Inorganic Chemistry, 2011, 2011, 4534-4544.	2.0	24

#	ARTICLE	IF	CITATIONS
523	Aerosolâ€Assisted CVD of Titanium Dioxide Thin Films from Methanolic Solutions of Titanium Tetraisopropoxide; Substrate and Aerosolâ€Selective Deposition of Rutile or Anatase. Chemical Vapor Deposition, 2011, 17, 30-36.	1.3	35
524	Textured Fluorineâ€Doped Tin Dioxide Films formed by Chemical Vapour Deposition. Chemistry - A European Journal, 2011, 17, 11613-11621.	3.3	56
525	Nanoparticulate silver coated-titania thin films—Photo-oxidative destruction of stearic acid under different light sources and antimicrobial effects under hospital lighting conditions. Journal of Photochemistry and Photobiology A: Chemistry, 2011, 220, 113-123.	3.9	69
526	Aerosol assisted deposition of melamine-formaldehyde resin: Hydrophobic thin films from a hydrophilic material. Thin Solid Films, 2011, 519, 2181-2186.	1.8	18
527	An investigation into bacterial attachment to an elastomeric superhydrophobic surface prepared via aerosol assisted deposition. Thin Solid Films, 2011, 519, 3722-3727.	1.8	181
528	Aerosol Assisted Depositions of Polymers Using an Atomiser Delivery System. Journal of Nanoscience and Nanotechnology, 2011, 11, 8358-8362.	0.9	4
529	Evaluating Zeolite-Modified Sensors: towards a faster set of chemical sensors. , 2011, , .		3
530	Enhanced Solubility and Covalent Functionalisation of Single Walled Carbon Nanotubes via Atmospheric Pressure Microwave Reflux and the Subsequent Spray Coating of Transparent Conducting Thin Films. Current Nanoscience, 2010, 6, 232-242.	1.2	5
531	Frictional properties of light-activated antimicrobial polymers in blood vessels. Journal of Materials Science: Materials in Medicine, 2010, 21, 815-821.	3.6	17
532	Antibacterial Activity of Light-Activated Silicone Containing Methylene Blue and Gold Nanoparticles of Different Sizes. Journal of Cluster Science, 2010, 21, 427-438.	3.3	62
533	Antimicrobial Activity in Thin Films of Pseudobrookiteâ€Structured Titanium Oxynitride under UV Irradiation Observed for <i>Escherichia coli</i> . Chemical Vapor Deposition, 2010, 16, 19-22.	1.3	16
534	Sulfur―and Nitrogenâ€Doped Titania Biomaterials via APCVD. Chemical Vapor Deposition, 2010, 16, 50-54.	1.3	34
535	Substrateâ€Dependant Ability of Titanium(IV) Oxide Photocatalytic Thin Films Prepared by Thermal CVD to Generate Hydrogen Gas from a Sacrificial Reaction. Chemical Vapor Deposition, 2010, 16, 301-304.	1.3	9
536	Atmospheric Pressure Chemical Vapour Deposition of TiCl <sub>4</sub> and <i>t</i> BuAsH <sub>2</sub> to Form Titanium Arsenide Thin Films. European Journal of Inorganic Chemistry, 2010, 2010, 5629-5634.	2.0	15
537	Preparation and Characterisation of Superâ€Hydrophobic Surfaces. Chemistry - A European Journal, 2010, 16, 3568-3588.	3.3	267
538	An Investigation into the Optimum Thickness of Titanium Dioxide Thin Films Synthesized by Using Atmospheric Pressure Chemical Vapour Deposition for Use in Photocatalytic Water Oxidation. Chemistry - A European Journal, 2010, 16, 10546-10552.	3.3	18
539	Atmospheric pressure chemical vapour deposition of NbSe2–TiSe2 composite thin films. Applied Surface Science, 2010, 256, 3178-3182.	6.1	10
540	Gas-sensing properties of Fe2â^'xTixO3+γ (x=0–1.4). Polyhedron, 2010, 29, 1225-1230.	2.2	7

#	Article	IF	CITATIONS
541	The combinatorial atmospheric pressure chemical vapour deposition (cAPCVD) of a gradating substitutional/interstitial N-doped anatase TiO2 thin-film; UVA and visible light photocatalytic activities. Journal of Photochemistry and Photobiology A: Chemistry, 2010, 216, 156-166.	3.9	60
542	Photocatalytic evolution of hydrogen and oxygen from ceramic wafers of commercial titanias. Journal of Photochemistry and Photobiology A: Chemistry, 2010, 216, 110-114.	3.9	19
543	Impaired bacterial attachment to light activated Ni–Ti alloy. Materials Science and Engineering C, 2010, 30, 225-234.	7.3	9
544	Superhydrophobic polymer films via aerosol assisted deposition — Taking a leaf out of nature's book. Thin Solid Films, 2010, 518, 4328-4335.	1.8	29
545	Nano-composite thermochromic thin films and their application in energy-efficient glazing. Solar Energy Materials and Solar Cells, 2010, 94, 141-151.	6.2	99
546	A comprehensive aerosol spray method for the rapid photocatalytic grid area analysis of semiconductor photocatalyst thin films. Analytica Chimica Acta, 2010, 663, 69-76.	5.4	24
547	Energy modelling studies of thermochromic glazing. Energy and Buildings, 2010, 42, 1666-1673.	6.7	175
548	The extended time evolution size decrease of gold nanoparticles formed by the Turkevich method. New Journal of Chemistry, 2010, 34, 1401.	2.8	38
549	High-Pressure Behavior and Polymorphism of Titanium Oxynitride Phase Ti <sub>2.85</sub> O <sub>4</sub> N. Journal of Physical Chemistry C, 2010, 114, 8546-8551.	3.1	8
550	The combinatorial atmospheric pressure chemical vapour deposition (cAPCVD) of a gradating N-doped mixed phase titania thin film. Journal of Materials Chemistry, 2010, 20, 2157.	6.7	48
551	Prevention of biofilm accumulation on a light-activated antimicrobial catheter material. Journal of Materials Chemistry, 2010, 20, 8668.	6.7	33
552	The effect of initiation method on the size, monodispersity and shape of gold nanoparticles formed by the Turkevich method. New Journal of Chemistry, 2010, 34, 2906.	2.8	37
553	The influence of a dc electric field on chemical interactions in "peroxide-metal―systems during combustion processes. New Journal of Chemistry, 2010, 34, 391.	2.8	1
554	Combinatorial atmospheric pressure chemical vapour deposition (cAPCVD) of niobium doped anatase; effect of niobium on the conductivity and photocatalytic activity. Journal of Materials Chemistry, 2010, 20, 8336.	6.7	53
555	Syntheses, X-ray structures and CVD of titanium(iv) arsine complexes. Dalton Transactions, 2010, 39, 5325.	3.3	12
556	Discrimination effects in zeolite modified metal oxide semiconductor gas sensors. , 2009, , .		1
557	Combinatorial CVD: New Oxynitride Photocatalysts. ECS Transactions, 2009, 25, 139-154.	O.5	7
558	Zeolite Modification: Towards Discriminating Metal Oxide Gas Sensors. ECS Transactions, 2009, 19, 241-250.	0.5	4

#	Article	IF	CITATIONS
559	Hybrid Aerosol Assisted Atmospheric Pressure Chemical Vapour Deposition: A Facile Route Toward Nano-Composite Thin Films?. ECS Transactions, 2009, 25, 773-780.	0.5	3
560	The Synthesis of Tantalum (V) Oxide Using Atmospheric Pressure Chemical Vapour Deposition for the Purposes of Photo-activated Water Splitting. ECS Transactions, 2009, 25, 935-942.	0.5	0
561	N-doped Titania Thin Films, Prepared by Atmospheric Pressure Chemical Vapour Deposition: Enhanced Visible Light Photocatalytic Activity and Anti-microbial Effects. ECS Transactions, 2009, 25, 65-72.	0.5	5
562	Combinatorial CVD: New Oxy-nitride Photocatalysts. ECS Transactions, 2009, 25, 1239-1250.	0.5	7
563	Use of hydroxypropylmethylcellulose 2% for removing adherent silicone oil from silicone intraocular lenses. British Journal of Ophthalmology, 2009, 93, 1085-1088.	3.9	10
564	A Single-Step Route Towards Large-Scale Deposition of Nanocomposite Thin Films Using Preformed Gold Nanoparticles. Materials Research Society Symposia Proceedings, 2009, 1174, 13.	0.1	0
565	Nâ€Doped Titania Thin Films Prepared by Atmospheric Pressure CVD using <i>t</i> â€Butylamine as the Nitrogen Source: Enhanced Photocatalytic Activity under Visible Light. Chemical Vapor Deposition, 2009, 15, 171-174.	1.3	31
566	Fabrication and characterization of Fe1.90Ti0.10O3 gas sensitive resistors for carbon monoxide. Sensors and Actuators B: Chemical, 2009, 135, 430-435.	7.8	8
567	Atmospheric pressure chemical vapour deposition of thermochromic tungsten doped vanadium dioxide thin films for use in architectural glazing. Thin Solid Films, 2009, 517, 4565-4570.	1.8	111
568	The antimicrobial properties of light-activated polymers containing methylene blue and gold nanoparticles. Biomaterials, 2009, 30, 89-93.	11.4	231
569	The Support Effect over Pt–H3PW12O40 Based Metal-Acid Bifunctional Catalysts on the Catalytic Performance in n-Pentane Isomerization. Catalysis Letters, 2009, 129, 215-221.	2.6	3
570	Templated growth of smart nanocomposite thin films: Hybrid aerosol assisted and atmospheric pressure chemical vapour deposition of vanadyl acetylacetonate, auric acid and tetraoctyl ammonium bromide. Polyhedron, 2009, 28, 2233-2239.	2.2	24
571	Ultra-violet light activated photocatalysis in thin films of the titanium oxynitride, Ti3â^î́O4N. Journal of Photochemistry and Photobiology A: Chemistry, 2009, 203, 199-203.	3.9	22
572	Titanium dioxide and composite metal/metal oxide titania thin films on glass: A comparative study of photocatalytic activity. Journal of Photochemistry and Photobiology A: Chemistry, 2009, 204, 183-190.	3.9	107
573	Enhanced photocatalytic activity under visible light in N-doped TiO2 thin films produced by APCVD preparations using t-butylamine as a nitrogen source and their potential for antibacterial films. Journal of Photochemistry and Photobiology A: Chemistry, 2009, 207, 244-253.	3.9	106
574	Nanoparticulate cerium dioxide and cerium dioxide–titanium dioxide composite thin films on glass by aerosol assisted chemical vapour deposition. Applied Surface Science, 2009, 256, 852-856.	6.1	18
575	Templated growth of smart coatings: Hybrid chemical vapour deposition of vanadyl acetylacetonate with tetraoctyl ammonium bromide. Applied Surface Science, 2009, 255, 7291-7295.	6.1	27
576	Features of power engineering in a dynamic electrically conductive medium. International Journal of Self-Propagating High-Temperature Synthesis, 2009, 18, 76-86.	0.5	0

#	Article	IF	CITATIONS
577	Simple method for the rapid simultaneous screening of photocatalytic activity over multiple positions of self-cleaning films. Physical Chemistry Chemical Physics, 2009, 11, 8367.	2.8	41
578	The interaction between gold nanoparticles and cationic and anionic dyes: enhanced UV-visible absorption. Physical Chemistry Chemical Physics, 2009, 11, 10513.	2.8	86
579	The role of surfaces in catheter-associated infections. Chemical Society Reviews, 2009, 38, 3435.	38.1	190
580	High-Throughput Continuous Hydrothermal Synthesis of an Entire Nanoceramic Phase Diagram. ACS Combinatorial Science, 2009, 11, 829-834.	3.3	65
581	The incorporation of noble metal nanoparticles into host matrix thin films: synthesis, characterisation and applications. Journal of Materials Chemistry, 2009, 19, 574-590.	6.7	173
582	White light induced photocatalytic activity of sulfur-doped TiO2 thin films and their potential for antibacterial application. Journal of Materials Chemistry, 2009, 19, 8747.	6.7	105
583	Antimicrobial surfaces and their potential in reducing the role of the inanimate environment in the incidence of hospital-acquired infections. Journal of Materials Chemistry, 2009, 19, 3819.	6.7	458
584	The reaction of tin(iv) iodide with phosphines: formation of new halotin anions. Dalton Transactions, 2009, , 10486.	3.3	10
585	Gas Sensing Properties of Composite Tungsten Trioxide-Zeolite Thick Films. ECS Transactions, 2009, 16, 77-84.	0.5	10
586	A single step route to superhydrophobic surfaces through aerosol assisted deposition of rough polymer surfaces: duplicating the lotus effect. Journal of Materials Chemistry, 2009, 19, 1074-1076.	6.7	49
587	Electromotive force measurements in the combustion wave front during layer-by-layer surface laser sintering of exothermic powder compositions. Physical Chemistry Chemical Physics, 2009, 11, 3503.	2.8	4
588	Combinatorial atmospheric pressure chemical vapour deposition (cAPCVD) of a mixed vanadium oxide and vanadium oxynitride thin film. Journal of Materials Chemistry, 2009, 19, 1399.	6.7	45
589	Antimicrobial activity of methylene blue and toluidine blue O covalently bound to a modified silicone polymer surface. Journal of Materials Chemistry, 2009, 19, 6167.	6.7	83
590	Carboxylic acid-stabilised iron oxide nanoparticles for use in magnetic hyperthermia. Journal of Materials Chemistry, 2009, 19, 6529.	6.7	126
591	Toluidine blue-containing polymers exhibit potent bactericidal activity when irradiated with red laser light. Journal of Materials Chemistry, 2009, 19, 2715.	6.7	59
592	Zeolite-Modified Discriminating Gas Sensors. Journal of the Electrochemical Society, 2009, 156, J46.	2.9	49
593	One-Step Synthesis of CuO Films Composed of Three-Dimensional Microflowers on Copper Surfaces. Journal of Nanoscience and Nanotechnology, 2009, 9, 1568-1570.	0.9	0
594	Enhancement by Nanogold of the Efficacy of a Light-Activated Antimicrobial Coating. Current Nanoscience, 2009, 5, 257-261.	1.2	6

#	Article	IF	CITATIONS
595	Synthesis and characterisation of W-doped VO2 by Aerosol Assisted Chemical Vapour Deposition. Thin Solid Films, 2008, 516, 1992-1997.	1.8	91
596	A Highly Effective Pt and H3PW12O40 Modified Zirconium Oxide Metal–Acid Bifunctional Catalyst for Skeletal Isomerization: Preparation, Characterization and Catalytic Behavior Study. Catalysis Letters, 2008, 125, 340-347.	2.6	7
597	Surface Laser Sintering of exothermic powder compositions. Journal of Thermal Analysis and Calorimetry, 2008, 91, 427-436.	3.6	21
598	Surfactant directed chemical vapour deposition of gold nanoparticles with narrow size distributions. Gold Bulletin, 2008, 41, 66-69.	2.7	27
599	An Investigation of Titaniumâ€Vanadium Nitride Phase Space, Conducted Using Combinatorial Atmospheric Pressure CVD. Chemical Vapor Deposition, 2008, 14, 309-312.	1.3	12
600	Zinc Oxide Thin Films Grown by Aerosol Assisted CVD. Chemical Vapor Deposition, 2008, 14, 366-372.	1.3	69
601	Atmospheric pressure chemical vapour deposition of SnSe and SnSe2 thin films on glass. Thin Solid Films, 2008, 516, 4750-4757.	1.8	156
602	SHS in the UK: Past, present, and future directions. International Journal of Self-Propagating High-Temperature Synthesis, 2008, 17, 266-274.	0.5	2
603	The gas-sensing properties of WO3â^'xthin films deposited via the atmospheric pressure chemical vapour deposition (APCVD) of WCl6with ethanol. Measurement Science and Technology, 2008, 19, 025203.	2.6	31
604	Gallium oxide thin films from the AACVD of [Ga(NMe2)3]2 and donor functionalised alcohols. Dalton Transactions, 2008, , 591.	3.3	44
605	CuO three-dimensional flowerlike nanostructures: Controlled synthesis and characterization. Journal of Applied Physics, 2008, 103, .	2.5	35
606	Porous biocompatible implants and tissue scaffolds synthesized by selective laser sintering from Ti and NiTi. Journal of Materials Chemistry, 2008, 18, 1309.	6.7	106
607	Chromium oxyselenide solid solutions from the atmospheric pressure chemical vapour deposition of chromyl chloride and diethylselenide. Journal of Materials Chemistry, 2008, 18, 1667.	6.7	15
608	Zeolite-based discriminating gas sensors. Studies in Surface Science and Catalysis, 2008, 174, 549-554.	1.5	4
609	Quantum dots as enhancers of the efficacy of bacterial lethal photosensitization. Nanotechnology, 2008, 19, 445102.	2.6	30
610	Design of Three-Dimensional Functional Articles via Layer-by-Layer Laser Sintering of Exothermic Powder Mixtures. Materials and Manufacturing Processes, 2008, 23, 571-578.	4.7	15
611	Gold Nanoparticles Enhance the Toluidine Blue-Induced Lethal Photosensitisation of Staphylococcus aureus. Current Nanoscience, 2008, 4, 409-414.	1.2	43
612	Zeolite Modified Discriminating Gas Sensors. ECS Transactions, 2008, 16, 275-286.	0.5	0

#	Article	IF	CITATIONS
613	Lethal photosensitisation of Staphylococcus aureus using a toluidine blue O–tiopronin–gold nanoparticle conjugate. Journal of Materials Chemistry, 2007, 17, 3739.	6.7	113
614	Photocatalytic Oxidation of Deposited Sulfur and Gaseous Sulfur Dioxide by TiO2 Films. Journal of Physical Chemistry C, 2007, 111, 5520-5525.	3.1	18
615	Aerosol-assisted chemical vapour deposition of WO3 thin films using polyoxometallate precursors and their gas sensing properties. Journal of Materials Chemistry, 2007, 17, 1063.	6.7	57
616	Aerosol assisted chemical vapour deposition of WO3 thin films from tungsten hexacarbonyl and their gas sensing properties. Journal of Materials Chemistry, 2007, 17, 3708.	6.7	64
617	Transition Metal Exchanged Zeolite Layers for Selectivity Enhancement of Metal-Oxide Semiconductor Gas Sensors. IEEE Sensors Journal, 2007, 7, 551-556.	4.7	26
618	Electrochemistry and Dynamic Ionography of Self-Propagating High-Temperature Synthesis (SHS). Materials Science Forum, 2007, 555, 73-81.	0.3	0
619	The effect of oxygen-containing reagents on the crystal morphology and orientation in tungsten oxide thin films deposited via atmospheric pressure chemical vapour deposition (APCVD) on glass substrates. Faraday Discussions, 2007, 136, 329.	3.2	16
620	The Use of Combinatorial Chemical Vapor Deposition in the Synthesis of Ti <sub>3</sub> <sub>-</sub> <sub>î</sub> O <sub>4</sub> N with 0.06 < δ < 0.25:  A Titanium Oxynitrio Phase Isostructural to Anosovite. Journal of the American Chemical Society, 2007, 129, 15541-15548.	de13.7	67
621	Aerosol Assisted Chemical Vapor Deposition of Gold and Nanocomposite Thin Films from Hydrogen Tetrachloroaurate(III). Chemistry of Materials, 2007, 19, 4639-4647.	6.7	63
622	A comparison of the gas sensing properties of solid state metal oxide semiconductor gas sensors produced by atmospheric pressure chemical vapour deposition and screen printing. Measurement Science and Technology, 2007, 18, 190-200.	2.6	32
623	Titania and silver–titania composite films on glass—potent antimicrobial coatings. Journal of Materials Chemistry, 2007, 17, 95-104.	6.7	304
624	Tungsten Oxide and Tungsten Oxide-Titania Thin Films Prepared by Aerosol-Assisted Deposition – Use of Preformed Solid Nanoparticles. European Journal of Inorganic Chemistry, 2007, 2007, 1415-1421.	2.0	17
625	Nb-Doped VO2 Thin Films Prepared by Aerosol-Assisted Chemical Vapour Deposition. European Journal of Inorganic Chemistry, 2007, 2007, 4050-4055.	2.0	77
626	Synthesis and Charaterisation of Chromium Oxyselenide (Cr2Se0.7O2.3) Formed from Chemical Vapour Synthesis: A New Antiferromagnet. European Journal of Inorganic Chemistry, 2007, 2007, 4579-4582.	2.0	7
627	Tungsten doped vanadium dioxide thin films prepared by atmospheric pressure chemical vapour deposition from vanadyl acetylacetonate and tungsten hexachloride. Surface and Coatings Technology, 2007, 201, 9369-9372.	4.8	43
628	A combinatorial approach to phase synthesis and characterisation in atmospheric pressure chemical vapour deposition. Surface and Coatings Technology, 2007, 201, 8966-8970.	4.8	14
629	Atmospheric pressure chemical vapour deposition of vanadium diselenide thin films. Applied Surface Science, 2007, 253, 6041-6046.	6.1	64
630	Synthesis and characterisation of titanium pyridine- and pyrimidine-thiolates and their application as precursors to titanium disulfide. Polyhedron, 2007, 26, 43-48.	2.2	15

#	Article	IF	CITATIONS
631	The APCVD of tungsten oxide thin films from reaction of WCl6 with ethanol and results on their gas-sensing properties. Polyhedron, 2007, 26, 1493-1498.	2.2	34
632	Phase composition and magnetism of combustion products in Ba–Fe–O compounds synthesized under applied DC electric field. Journal of Magnetism and Magnetic Materials, 2007, 309, 202-206.	2.3	4
633	Damaging and protective properties of inorganic components of sunscreens applied to cultured human skin cells. Journal of Photochemistry and Photobiology A: Chemistry, 2007, 191, 138-148.	3.9	53
634	Aerosol assisted chemical vapour deposition of MoO3 and MoO2 thin films on glass from molybdenum polyoxometallate precursors; thermophoresis and gas phase nanoparticle formation. Journal of Materials Chemistry, 2006, 16, 3575.	6.7	55
635	Chemical vapour deposition of titanium chalcogenides and pnictides and tungsten oxide thin films. New Journal of Chemistry, 2006, 30, 505.	2.8	30
636	Atmospheric pressure chemical vapor deposition of WSe2thin films on glass—highly hydrophobic sticky surfaces. Journal of Materials Chemistry, 2006, 16, 122-127.	6.7	128
637	X-ray Diffraction Area Mapping of Preferred Orientation and Phase Change in TiO2Thin Films Deposited by Chemical Vapor Deposition. Journal of the American Chemical Society, 2006, 128, 12147-12155.	13.7	65
638	Intelligent Thermochromic Windows. Journal of Chemical Education, 2006, 83, 393.	2.3	162
639	High Conductivity La2-xSrxCu1-y(Mg, Al)yO4Solid State Metal Oxide Gas Sensors with the K2NiF4Structure. Chemistry of Materials, 2006, 18, 3351-3355.	6.7	26
640	Aerosol Assisted Chemical Vapor Deposition Using Nanoparticle Precursors:Â A Route to Nanocomposite Thin Films. Journal of the American Chemical Society, 2006, 128, 1587-1597.	13.7	151
641	Composite thermochromic thin films: (TiO2)–(VO2) prepared from titanium isopropoxide, VOCl3 and water. Polyhedron, 2006, 25, 334-338.	2.2	20
642	Antimony oxide thin films from the atmospheric pressure chemical vapour deposition reaction of antimony pentachloride and ethyl acetate. Polyhedron, 2006, 25, 3032-3038.	2.2	20
643	Combustion synthesis of sodium-substituted lanthanum manganites. Mendeleev Communications, 2006, 16, 36-38.	1.6	2
644	Atmospheric Pressure Chemical Vapour Deposition of NbSe2 Thin Films on Glass. European Journal of Inorganic Chemistry, 2006, 2006, 1255-1259.	2.0	48
645	Platin-Komplexe der Anionen Se2N 22⊗ und Se2N2H⊗; Röntgenstrukturanalyse von [Pt(Se2N2H)(PMe2Ph)2]Cl. Angewandte Chemie, 2006, 101, 1052-1053.	2.0	10
646	Advanced Ways and Experimental Methods in Self-Propagating High-Temperature Synthesis (SHS) of Inorganic Materials. Materials Science Forum, 2006, 518, 181-188.	0.3	11
647	Synthesis and properties of nickel–cobalt–boron nanoparticles. Journal of Physics: Conference Series, 2005, 17, 196-200.	0.4	1
648	Molecular precursors for the CVD of niobium and tantalum nitride. Polyhedron, 2005, 24, 463-468.	2.2	23

#	Article	IF	CITATIONS
649	Aerosol-Assisted Chemical Vapor Deposition of NbS2 and TaS2 Thin Films from Pentakis(dimethylamido)metal Complexes and 2-Methylpropanethiol. European Journal of Inorganic Chemistry, 2005, 2005, 4179-4185.	2.0	32
650	Particle Size and Oxidation in CoNi Nanoparticles. Materials Research Society Symposia Proceedings, 2005, 877, 1.	0.1	1
651	Self-cleaning coatings. Journal of Materials Chemistry, 2005, 15, 1689.	6.7	855
652	Control of semiconducting oxide gas-sensor microstructure by application of an electric field during aerosol-assisted chemical vapour deposition. Journal of Materials Chemistry, 2005, 15, 149.	6.7	37
653	Reactivity of tetrakisdimethylamido-titanium(iv) and -zirconium(iv) with thiols. New Journal of Chemistry, 2005, 29, 620.	2.8	8
654	Synthesis and characterisation of tungsten(vi) oxo-salicylate complexes for use in the chemical vapour deposition of self-cleaning films. Dalton Transactions, 2005, , 1287.	3.3	9
655	Synthesis of Titanium(IV) Guanidinate Complexes and the Formation of Titanium Carbonitride via Low-Pressure Chemical Vapor Deposition. Inorganic Chemistry, 2005, 44, 615-619.	4.0	60
656	APCVD of thermochromic vanadium dioxide thin films—solid solutions V2–xMxO2 (M = Mo, Nb) or composites VO2 : SnO2. Journal of Materials Chemistry, 2005, 15, 4560.	6.7	93
657	Metal oxide semiconductor gas sensors utilizing a Cr-zeolite catalytic layer for improved selectivity. Measurement Science and Technology, 2005, 16, 1193-1200.	2.6	41
658	Atmospheric Pressure Chemical Vapor Deposition of Crystalline Monoclinic WO3 and WO3-x Thin Films from Reaction of WCl6 with O-Containing Solvents and Their Photochromic and Electrochromic Properties. Chemistry of Materials, 2005, 17, 1583-1590.	6.7	161
659	Intelligent Window Coatings: Atmospheric Pressure Chemical Vapor Deposition of Tungsten-Doped Vanadium Dioxide ChemInform, 2004, 35, no.	0.0	4
660	NbS2 thin films by atmospheric pressure chemical vapour deposition and the formation of a new 1T polytype. Thin Solid Films, 2004, 469-470, 495-499.	1.8	11
661	Aerosol-assisted chemical vapour deposition of sodium fluoride thin films. Thin Solid Films, 2004, 469-470, 416-419.	1.8	24
662	Vanadium(IV) oxide thin films on glass and silicon from the atmospheric pressure chemical vapour deposition reaction of VOCl3 and water. Polyhedron, 2004, 23, 3087-3095.	2.2	73
663	Low temperature deposition of crystalline chromium phosphide films using dual-source atmospheric pressure chemical vapour deposition. Applied Surface Science, 2004, 233, 24-28.	6.1	12
664	The reaction of GeCl4 with primary and secondary phosphines. Dalton Transactions, 2004, , 470.	3.3	15
665	Combustion synthesis of alkaline-earth substituted lanthanum manganites; LaMnO3, La0.6Ca0.4MnO3 and La0.6Sr0.4MnO3. Journal of Materials Chemistry, 2004, 14, 1377.	6.7	21
666	Formation of a new (1T) trigonal NbS2 polytype via atmospheric pressure chemical vapour depositionElectronic supplementary information (ESI) available: structure refinements of the NbS2 films and crystallographic data in CIF format. See http://www.rsc.org/suppdata/jm/b3/b315782m/. Journal of Materials Chemistry, 2004, 14, 290.	6.7	42

#	Article	IF	CITATIONS
667	Dual source APCVD synthesis of TaN and NbN thin films on glass from the reaction of MCl5 (M = Ta,) Tj ETQq1 1	0.784314	rgBT /Overlo
668	Dual-source chemical vapour deposition of titanium sulfide thin films from tetrakisdimethylamidotitanium and sulfur precursors. Journal of Materials Chemistry, 2004, 14, 3474.	6.7	28
669	Aerosol assisted chemical vapour deposition of photochromic tungsten oxide and doped tungsten oxide thin films. Journal of Materials Chemistry, 2004, 14, 2864.	6.7	79
670	Laser-induced combustion synthesis of 3D functional materials: computer-aided design. Journal of Materials Chemistry, 2004, 14, 3444.	6.7	25
671	Titanium sulfide thin films from the aerosol-assisted chemical vapour deposition of [Ti(SBut)4]. Journal of Materials Chemistry, 2004, 14, 830.	6.7	39
672	Atmospheric pressure chemical vapour deposition of tungsten doped vanadium(iv) oxide from VOCl3, water and WCl6. Journal of Materials Chemistry, 2004, 14, 2554.	6.7	119
673	Gallium Oxide Thin Films from the Atmospheric Pressure Chemical Vapor Deposition Reaction of Gallium Trichloride and Methanol. Chemistry of Materials, 2004, 16, 2489-2493.	6.7	67
674	Atmospheric pressure chemical vapour deposition of VO2 and VO2/TiO2 films from the reaction of VOCl3, TiCl4 and water. Journal of Materials Chemistry, 2004, 14, 1190.	6.7	58
675	Intelligent Window Coatings:Â Atmospheric Pressure Chemical Vapor Deposition of Tungsten-Doped Vanadium Dioxide. Chemistry of Materials, 2004, 16, 744-749.	6.7	363
676	Self propagating high temperature synthesis of magnesium zinc ferrites (MgxZn1 â~` xFe2O3): thermal imaging and time resolved X-ray diffraction experiments. Journal of Materials Chemistry, 2004, 14, 1104-1111.	6.7	21
677	Atmospheric-Pressure Chemical Vapor Deposition of Group IVb Metal Phosphide Thin Films from Tetrakisdimethylamidometal Complexes and Cyclohexylphosphine. Chemistry of Materials, 2004, 16, 1120-1125.	6.7	19
678	Anatase Thin Films on Glass from the Chemical Vapor Deposition of Titanium(IV) Chloride and Ethyl Acetate ChemInform, 2003, 34, no.	0.0	0
679	Solvent-Free Reactions in the Solid State: Solid State Metathesis. ChemInform, 2003, 34, no.	0.0	0
680	Dual-source chemical vapour deposition of titanium(III) phosphide from titanium tetrachloride and tristrimethylsilylphosphine. Applied Surface Science, 2003, 211, 2-5.	6.1	9
681	Titania and tungsten doped titania thin films on glass; active photocatalysts. Polyhedron, 2003, 22, 35-44.	2.2	150
682	Atmospheric pressure chemical vapour deposition of TiS2 thin films on glass. Polyhedron, 2003, 22, 1263-1269.	2.2	28
683	The use of hexamethyldisilathiane for the synthesis of transition metal sulfides. Polyhedron, 2003, 22, 1255-1262.	2.2	9
684	Atmospheric pressure chemical vapour deposition of WS2 thin films on glass. Polyhedron, 2003, 22, 1499-1505.	2.2	67

#	Article	IF	CITATIONS
685	Germanium phosphide coatings from the atmospheric pressure chemical vapour deposition of GeX4 (X=Cl or Br) and PCychexH2. Polyhedron, 2003, 22, 1683-1688.	2.2	8
686	Characterisation of the photocatalyst Pilkington Activâ,,¢: a reference film photocatalyst?. Journal of Photochemistry and Photobiology A: Chemistry, 2003, 160, 213-224.	3.9	283
687	Thick titanium dioxide films for semiconductor photocatalysis. Journal of Photochemistry and Photobiology A: Chemistry, 2003, 160, 185-194.	3.9	194
688	Atmospheric pressure chemical vapour deposition of thin films of Nb2O5 on glass. Journal of Materials Chemistry, 2003, 13, 2952.	6.7	40
689	Atmospheric pressure chemical vapour deposition of titanium dioxide coatings on glass. Journal of Materials Chemistry, 2003, 13, 56-60.	6.7	74
690	Anatase Thin Films on Glass from the Chemical Vapor Deposition of Titanium(IV) Chloride and Ethyl Acetate. Chemistry of Materials, 2003, 15, 46-50.	6.7	72
691	Tungsten Oxide Coatings from the Aerosol-Assisted Chemical Vapor Deposition of W(OAr)6(Ar = C6H5,) Tj ETQq1	1 0.7843 6.7	314 rgBT /O
692	Synthesis of TiN thin films from titanium imido complexes. Journal of Materials Chemistry, 2003, 13, 84-87.	6.7	43
693	Aerosol assisted chemical vapour deposition of tungsten oxide films from polyoxotungstate precursors: active photocatalysts. Chemical Communications, 2003, , 1696.	4.1	53
694	Chemical vapour deposition of group Vb metal phosphide thin films. Journal of Materials Chemistry, 2003, 13, 1930.	6.7	16
695	Atmospheric pressure chemical vapour deposition of Cr2â^'xTixO3(CTO) thin films (â‰ <b>s</b> Âμm) on to gas sensing substrates. Journal of Materials Chemistry, 2003, 13, 2957-2962.	6.7	22
696	Heterogeneous combustion in electrical and magnetic fields: modification of combustion parameters and products. Physical Chemistry Chemical Physics, 2003, 5, 2291-2296.	2.8	11
697	A simple equivalent circuit model to represent microstructure effects on the response of semiconducting oxide-based gas sensors. Measurement Science and Technology, 2003, 14, 76-86.	2.6	42
698	Synthesis of a Homoleptic Niobium(V) Thiolate Complex and the Preparation of Niobium Sulfide via Thio "Solâ^'Gel―and Vapor Phase Thin-Film Experiments. Inorganic Chemistry, 2002, 41, 3668-3672.	4.0	24
699	The dual source APCVD of titanium nitride thin films from reaction of hexamethyldisilazane and titanium tetrachloride. Journal of Materials Chemistry, 2002, 12, 1906-1909.	6.7	33
700	Spectral and photocatalytic characteristics of TiO2 CVD films on quartz. Photochemical and Photobiological Sciences, 2002, 1, 865-868.	2.9	74
701	Single-source CVD routes to titanium phosphide. Dalton Transactions RSC, 2002, , 2702-2709.	2.3	23
702	Titanium Phosphide Coatings from the Atmospheric Pressure Chemical Vapor Deposition of TiCl4and RPH2(R =t-Bu, Ph, CyHex). Chemistry of Materials, 2002, 14, 3167-3173.	6.7	20

#	Article	IF	CITATIONS
703	Synthesis and thermal decomposition studies of homo- and heteroleptic tin(iv) thiolates and dithiocarbamates: molecular precursors for tin sulfides. Dalton Transactions RSC, 2002, , 1085-1092.	2.3	71
704	Intelligent window coatings: atmospheric pressure chemical vapour deposition of vanadium oxides. Journal of Materials Chemistry, 2002, 12, 2936-2939.	6.7	220
705	Titanium imido complexes as precursors to titanium nitride. Dalton Transactions RSC, 2002, , 4055-4059.	2.3	35
706	Novel TiO2 CVD films for semiconductor photocatalysis. Journal of Photochemistry and Photobiology A: Chemistry, 2002, 151, 171-179.	3.9	215
707	Solid state metathesis synthesis of metal silicides; reactions of calcium and magnesium silicide with metal oxides. Polyhedron, 2002, 21, 187-191.	2.2	29
708	Tin phosphide coatings from the atmospheric pressure chemical vapour deposition of SnX4 (X=Cl or) Tj ETQq0 C	0 0 <u>rg</u> BT /C	Overlock 10 Tf
709	Self-propagating solid state routes to BaSnO3; investigation of gas sensing properties. Journal of Materials Science, 2002, 37, 375-379.	3.7	18
710	Solvent free reactions in the solid state: solid state metathesis. Transition Metal Chemistry, 2002, 27, 569-573.	1.4	36
711	Exchange-Driven Magnetic Anomalies in Fe–Zr–B-Based Nanocomposites. Hyperfine Interactions, 2002, 144/145, 223-230.	0.5	1
712	Solid state synthesis of binary metal chalcogenides. Dalton Transactions RSC, 2001, , 1872-1875.	2.3	16
713	Liquid Ammonia Mediated Metathesis:Â Synthesis of Binary Metal Chalcogenides and Pnictides. Inorganic Chemistry, 2001, 40, 6940-6947.	4.0	17
714	Self-propagating high-temperature synthesis of chromium substituted lanthanum orthoferrites LaFe1 Ⱂ xCrxO3 (0 ≤ ≤). Journal of Materials Chemistry, 2001, 11, 854-858.	6.7	31
715	Deposition of tin sulfide thin films from tin(iv) thiolate precursors. Journal of Materials Chemistry, 2001, 11, 464-468.	6.7	65
716	Deposition of tin sulfide thin films from novel, volatile (fluoroalkythiolato)tin(iv) precursors. Journal of Materials Chemistry, 2001, 11, 469-473.	6.7	74
717	Microspheres of the gas sensor material Cr2 â^ xTixO3 prepared by the sol–emulsion–gel route. Journal of Materials Chemistry, 2001, 11, 1651-1655.	6.7	35
718	Dual source atmospheric pressure chemical vapour deposition of TiP films on glass using TiCl4 and PH2But. Journal of Materials Chemistry, 2001, 11, 2408-2409.	6.7	18
719	Solid state metathesis: synthesis of metal carbides from metal oxides. Journal of Materials Chemistry, 2001, 11, 3116-3119.	6.7	69
720	Thiolate derivatives of titanium(iv) and tantalum(v) as precursors to metal sulfides. Dalton Transactions RSC, 2001, , 2554-2558.	2.3	18

#	Article	IF	CITATIONS
721	Self-propagating high temperature synthesis of BaFe12O19, Mg0.5Zn0.5Fe2O4 and Li0.5Fe2.5O4; time resolved X-ray diffraction studies (TRXRD). Journal of Materials Chemistry, 2001, 11, 193-199.	6.7	22
722	Structural distortions in homoleptic (RE)4A (E = O, S, Se; A = C, Si, Ge, Sn): implications for the CVD of tin sulfides. Dalton Transactions RSC, 2001, , 3435-3445.	2.3	16
723	Title is missing!. Journal of Materials Chemistry, 2001, 11, 3120-3124.	6.7	47
724	The first single source deposition of tin sulfide coatings on glass: aerosol-assisted chemical vapour deposition using [Sn(SCH2CH2S)2]. Journal of Materials Chemistry, 2001, 11, 1486-1490.	6.7	115
725	Self-propagating high temperature synthesis of MFe12O19 (M=Sr,Ba) from the reactions of metal superoxides and iron metal. Journal of Materials Processing Technology, 2001, 110, 239-243.	6.3	24
726	Novel SHS routes to CoTi-doped M-type ferrites. Journal of Materials Science: Materials in Electronics, 2001, 12, 533-536.	2.2	5
727	Combined combustion sol-gel synthesis of LiNbO3, LiTaO3, NaNbO3 and NaTaO3. Journal of Materials Science Letters, 2001, 20, 57-58.	0.5	11
728	DESIGNING PRECURSORS FOR THE DEPOSITION OF TIN SULPHIDE THIN FILMS. Main Group Metal Chemistry, 2001, 24, .	1.6	3
729	Atmospheric-Pressure CVD of Vanadium Oxynitride on Glass: Potential Solar Control Coatings. Chemical Vapor Deposition, 2000, 6, 59-63.	1.3	9
730	Combustion Synthesis of BaFe12O19 in an External Magnetic Field: Time-Resolved X-ray Diffraction (TRXRD) Studies. Advanced Materials, 2000, 12, 1359-1362.	21.0	23
731	Liquid-mediated metathetical synthesis of binary and ternary transition-metal pnictides. Polyhedron, 2000, 19, 829-833.	2.2	15
732	Self-propagating high temperature synthesis of yttrium iron chromium garnets Y3Fe5 â^' xCrxO12 (0 ≤x) Tj E	ГQq0,00r 8.7	rgBT /Overloc
733	Thio sol–gel synthesis of titanium disulfide from titanium thiolates. Journal of Materials Chemistry, 2000, 10, 2823-2826.	6.7	19
734	Bulk magnetization of the heavy rare earth titanate pyrochlores - a series of model frustrated magnets. Journal of Physics Condensed Matter, 2000, 12, 483-495.	1.8	167
735	Synthesis and Characterization of a Homoleptic Thiolate Complex of Titanium(IV). Inorganic Chemistry, 2000, 39, 2693-2695.	4.0	16
736	Atmospheric pressure chemical vapour deposition of tin(ii) sulfide films on glass substrates from Bun3SnO2CCF3 with hydrogen sulfide. Journal of Materials Chemistry, 2000, 10, 527-530.	6.7	47
737	The effect of large magnetic fields on solid state combustion reactions: novel microstructure, lattice contraction and reduced coercivity in barium hexaferrite. Journal of Materials Chemistry, 2000, 10, 235-237.	6.7	24
738	Atmospheric pressure chemical vapour deposition of vanadium(v) oxide films on glass substrates from reactions of VOCl3 and VCl4 with water. Journal of Materials Chemistry, 2000, 10, 1863-1866.	6.7	41

#	Article	IF	CITATIONS
739	Synthesis and structural characterisation of titanium(IV) thiolate compounds. Dalton Transactions RSC, 2000, , 3500-3504.	2.3	4
740	Microstructural aspects of the self-propagating high temperature synthesis of hexagonal barium ferrites in an external magnetic field. Journal of Materials Chemistry, 2000, 10, 1925-1932.	6.7	33
741	Self-propagating high-temperature synthesis of barium-chromium ferrites BaFe12-xCrxO19(0lexle6.0). Journal Physics D: Applied Physics, 1999, 32, 2590-2598.	2.8	31
742	Preparation of Fe–Zr–B amorphous alloys by chemical reduction. Journal of Materials Processing Technology, 1999, 92-93, 525-528.	6.3	10
743	Synthesis of Amorphous Fe-Zr-B by Chemical Reduction. Journal of Materials Science Letters, 1999, 18, 425-426.	0.5	0
744	Fast Metathesis Routes to Tungsten and Molybdenum Carbides. , 1999, 18, 267-268.		11
745	Preparation of FeMnB Alloys by Chemical Reduction. Journal of Materials Science Letters, 1999, 18, 39-40.	0.5	2
746	Self propagating high temperature synthesis of BaFe12â^'xCrxO19 and Li0.5Fe2.5â^'xCrxO4. Journal of Materials Chemistry, 1999, 9, 273-281.	6.7	16
747	Solid state metathesis routes to transition metal carbides. Journal of Materials Chemistry, 1999, 9, 1275-1281.	6.7	138
748	Combustion synthesis of chromium-substituted lithium ferrites Li0.5Fe2.5â^'xCrxO4 (xâ‰ <b>û</b> .0): Rietveld analysis and magnetic measurements. Solid State Sciences, 1999, 1, 311-316.	0.7	21
749	Atmospheric Pressure Chemical Vapor Deposition of Tin Sulfides (SnS, Sn2S3, and SnS2) on Glass. Chemistry of Materials, 1999, 11, 1792-1799.	6.7	377
750	Sodium borohydride reduction of aqueous iron–zirconium solutions: chemical routes to amorphous and nanocrystalline Fe–Zr–B alloys. Journal of Materials Chemistry, 1999, 9, 2537-2544.	6.7	21
751	Selfâ€propagating highâ€temperature synthesis of ferrites MFe2O4 (M = Mg, Ba, Co, Ni, Cu, Zn); reactions in an external magnetic field. Journal of Materials Chemistry, 1999, 9, 2545-2552.	6.7	129
752	Rapid, Solid-State Metathesis Routes to Metal Carbides. Advanced Materials, 1998, 10, 805-808.	21.0	47
753	Atmospheric Pressure CVD of SnS and SnS <sub>2</sub> on Glass. Chemical Vapor Deposition, 1998, 4, 222-225.	1.3	14
754	Solid-state and solution phase metathetical synthesis of copper indium chalcogenides. Journal of Materials Chemistry, 1998, 8, 2209-2211.	6.7	25
755	Chromium nitrides (CrN, Cr2N) from solid state metathesis reactions: effects of dilution and nitriding reagent. Journal of Materials Chemistry, 1998, 8, 1875-1880.	6.7	34
756	Convenient, low energy routes to hexagonal ferrites MFe12O19(M=Sr, Ba) from SHS reactions of iron, iron oxide and MO2 in air. Journal of Materials Chemistry, 1998, 8, 573-578.	6.7	21

#	Article	IF	CITATIONS
757	Self propagating high-temperature synthesis of chromium substituted magnesium zinc ferrites Mg0.5Zn0.5Fe2â"xCrxO4 (0≤â‰⊉.5). Journal of Materials Chemistry, 1998, 8, 2701-2706.	6.7	13
758	Self-propagating high-temperature synthesis of lithium-chromium ferrites Li0.5Fe2.5-xCrxO4. Journal Physics D: Applied Physics, 1998, 31, 2886-2893.	2.8	40
759	Rapid, Solid-State Metathesis Routes to Metal Carbides. , 1998, 10, 805.		1
760	Rapid, Solid-State Metathesis Routes to Metal Carbides. Advanced Materials, 1998, 10, 805-808.	21.0	1
761	Preparation and Characterization of a Material of Composition BiP (Bismuth Phosphide) and Other Intergroup 15 Element Phases. Chemistry of Materials, 1997, 9, 1385-1392.	6.7	32
762	Solid state metathesis routes to metal nitrides; use of strontium and barium nitrides as reagents and dilution effects. Polyhedron, 1997, 16, 3635-3640.	2.2	14
763	Self-Propagating High Temperature Synthesis of Hexagonal Ferrites MFe12O19 (M = Sr, Ba). Advanced Materials, 1997, 9, 643-645.	21.0	30
764	Room Temperature Synthesis in Liquid Ammonia of Zinc, Cadmium, and Mercury Sulfides. Main Group Chemistry, 1996, 1, 183-187.	0.8	7
765	New routes in the self-propagating high-temperature synthesis of barium titanium oxide. Polyhedron, 1996, 15, 1349-1353.	2.2	13
766	Self-propagating high-temperature synthesis of SrTiO3 and SrxBayTiO3 (x+y=1). Journal of Materials Science, 1996, 31, 5033-5037.	3.7	13
767	Elemental, liquid ammonia facilitated routes to zinc, cadmium, mercury copper, silver and lead telluride. Journal of Materials Science Letters, 1996, 15, 1741-1742.	0.5	24
768	Self propagating high temperature synthesis of BaTiO3 using titanium trichloride as a fuel source. Journal of Materials Science Letters, 1996, 15, 542-543.	0.5	5
769	The anhydrous alums as model triangular-lattice magnets. Journal of Physics Condensed Matter, 1996, 8, L123-L129.	1.8	36
770	Sodium azide as a reagent for solid state metathesis preparations of refractory metal nitrides. Polyhedron, 1995, 14, 913-917.	2.2	41
771	SYNTHESIS OF METAL SILICIDE POWDERS BY THERMOLYSIS OF METAL CHLORIDES WITH MAGNESIUM SILICIDE. Phosphorus, Sulfur and Silicon and the Related Elements, 1995, 101, 47-55.	1.6	13
772	Formation of transition-metal nitrides from the reactions of lithium amides and anhydrous transition-metal chlorides. Journal of Materials Chemistry, 1995, 5, 909.	6.7	25
773	Transition Metal Pnictide Synthesis: Self Propagating Reactions Involving Sodium Arsenide, Antimonide and Bismuthide. Zeitschrift Fur Naturforschung - Section B Journal of Chemical Sciences, 1994, 49, 477-482.	0.7	14
774	SELF PROPAGATING ROUTES TO GALLIUM AND INDIUM CHALCOGENIDES. Main Group Metal Chemistry, 1994, 17, .	1.6	9

#	Article	IF	CITATIONS
775	Low-energy initiated routes to crystalline metal phosphides and arsenides. Journal of Materials Science Letters, 1994, 13, 1-2.	0.5	9

## A convenient route to crystalline LiLnS2 (Ln = Nd, Sm, Gd, Tb, Dy, Ho, Er, Yb) and Ln x ,S y (Ln = La, Ce,) Tj ETQq0 0 0 ggBT /Overlock 10

777	Metathetical routes to uranium and thorium oxides and nitrides. Journal of Materials Science Letters, 1994, 13, 1185-1186.	0.5	8
778	Solid state metathesis preparations of group VIII metal oxide powders. Journal of Materials Science Letters, 1994, 13, 219-221.	0.5	5
779	Self-propagating routes to transition-metal phosphides. Journal of Materials Chemistry, 1994, 4, 279.	6.7	31
780	New routes to alkali-metal–rare-earth-metal sulfides. Journal of Materials Chemistry, 1994, 4, 1603-1609.	6.7	66
781	Metathesis routes to lanthanide pnictides. Journal of Materials Chemistry, 1994, 4, 285.	6.7	14
782	A synthesis of bismuth(III) phosphide: the first binary phosphide of bismuth. Journal of the Chemical Society Chemical Communications, 1994, , 1987.	2.0	11
783	Tungsten(6+) Tris(pinacolate): Structure and Comments on the Preference for an Octahedral Geometry Relative to Trigonal Prismatic (D3h) for a d0 Complex in the Presence of Strong .piDonor Ligands. Inorganic Chemistry, 1994, 33, 812-815.	4.0	21
784	A convenient low temperature route to the formation of lanthanide oxides. Inorganica Chimica Acta, 1993, 211, 77-80.	2.4	17
785	A convenient, rapid, low-energy route to crystalline TIN, VN and Ti x V y N (x + y = 1). Journal of Materials Science Letters, 1993, 12, 1856-1857.	0.5	5
786	Synthesis and characterization of M2(EPh3)2(NMe2)4 compounds (E = C, Si, Ge, Sn; M = Mo, W). Polyhedron, 1993, 12, 961-965.	2.2	11
787	Low-temperature routes to early transition-metal nitrides. Journal of the Chemical Society Dalton Transactions, 1993, , 2435.	1.1	48
788	Convenient, low energy, solid–liquid metathesis reactions; synthesis of TiN, TiO2, VN, VO2and TixVyN (x+y= 1). Journal of the Chemical Society Chemical Communications, 1993, .	2.0	15
789	Convenient synthesis of lanthanide and mixed lanthanide phosphides by solid-state routes involving sodium phosphide. Journal of Materials Chemistry, 1993, 3, 689.	6.7	30
790	Homoleptic optically active ditungsten and dimolybdenum alkoxides. The crystal structure of (+)[W2(OC10H19)6]. Journal of the Chemical Society Dalton Transactions, 1992, , 2343.	1.1	10
790 791	Homoleptic optically active ditungsten and dimolybdenum alkoxides. The crystal structure of (+)[W2(OC10H19)6]. Journal of the Chemical Society Dalton Transactions, 1992, , 2343. Diolates of dimolybdenum and ditungsten (MM) with seven-, eight- and nine-membered rings. Journal of the Chemical Society Chemical Communications, 1991, , 1673-1675.	1.1 2.0	10 15

#	Article	IF	CITATIONS
793	Mixed alkoxide-anilide d3-d3 dimers of molybdenum and tungsten. The X-ray crystal structures of M2(OBut)4(HNPh)2(H2NPh)2 (M = Mo, W). Polyhedron, 1991, 10, 2309-2316.	2.2	10
794	REACTION OF Pt(Se2N2)(DPPE) WITH HALOGENS: A NEW ROUTE TO Se4N4. THE X-RAY CRYSTAL STRUCTURE OF 3[PtI2(DPPE)]·I2·2[CH2C2]. Phosphorus, Sulfur and Silicon and the Related Elements, 1991, 57, 273-277.	1.6	12
795	The preparation and characterization of Pt(Se3PPh)(PR3)2; the X-ray crystal structure of Pt(Se3PPh)(dppe)·CH2Cl2. Polyhedron, 1990, 9, 987-990.	2.2	33
796	Preparation and characterization of M2(SeAr′)6 and mixed ligand M2(OR)2(SeAr′)4 species (M = Mo, W). Polyhedron, 1990, 9, 2941-2952.	2.2	13
797	The preparation and x-ray characterisation of [(PPh2Me)2Pt(μ-PPhH)2Pt(PPh2Me)2] [Cl]4·CH2Cl2 and [(PPh2Me)2Pt(μ-PPhH)Pt(PPh2Me)2] [Cl]2 [PhPO2OH]2 [PhPO(OH)2]2. Inorganica Chimica Acta, 1990, 172, 159-163.	2.4	14
798	NEW SYNTHETIC ROUTES TO S <sub>4</sub> N <sub>4</sub> and S <sub>7</sub> NH. REACTION OF Li <sub>3</sub> N WITH S <sub>3</sub> N <sub>3</sub> Cl <sub>3</sub> AND SCl <sub>2</sub> . Phosphorus, Sulfur and Silicon and the Related Elements, 1990, 47, 141-143.	1.6	2
799	Preparation and properties of [M{S2N3(SO2NH2)}(PR3)2] and [Pt{SO2(NH)2}(PR3)2] from reactions in liquid ammonia. Journal of the Chemical Society Dalton Transactions, 1990, , 519.	1.1	15
800	Triple bonds between molybdenum and tungsten atoms supported by selenolate ligands: M2(SeAr)6 and M2(OPri)2(SeAr)4(Ar = mesityl). Journal of the Chemical Society Chemical Communications, 1990, , 920.	2.0	9
801	Preparation and characterisation of [Pt(SeSN2)(PR3)2], [Pt(Se2N2)(PR3)2], [Pt(SeSN2H)(PR3)2]BF4, and [Pt(Se2N2H)(PR3)2]BF4. Journal of the Chemical Society Dalton Transactions, 1990, , 925.	1.1	9
802	Nitrogen-14 nuclear magnetic resonance studies on sulphur–nitrogen compounds. Journal of the Chemical Society Dalton Transactions, 1990, , 511-517.	1.1	12
803	Metalla-Sulphur-Nitrogen Chemistry. Phosphorus, Sulfur and Silicon and the Related Elements, 1989, 41, 223-228.	1.6	0
804	Platinum Complexes of the Anions Se2N22? and Se2N2H?; X-Ray Structure Analysis of [Pt(Se2N2H) (PMe2Ph)2]Cl. Angewandte Chemie International Edition in English, 1989, 28, 1047-1049.	4.4	21
805	Preparation and ligand properties of bis-thionylimino complexes of the type M(NSO)2(PR3)2. X-ray structure of Pt(NSO)2(PMe3)2. Polyhedron, 1989, 8, 835-839.	2.2	21
806	Bridging amido complexes from reactions in liquid ammonia. X-ray crystal structure of [Pt(PMe2Ph)2(μ-NH2)2Pt(PMe2Ph)2](BF4)2. Polyhedron, 1989, 8, 1979-1981.	2.2	15
807	Synthesis and properties of bis-imido complexes of the type Pt(NH)2C6H3NO2(PR3)2 from reactions in liquid ammonia. X-ray structure of Pt(NH)2C6H3NO2(PMePh2)2. Polyhedron, 1989, 8, 2507-2511.	2.2	3
808	The preparation and X-ray structures of Pt(SeSN2)(PMe2Ph)2 and [Pt(SeSN2H)(PMe2Ph)2]BF4. Polyhedron, 1989, 8, 2215-2217.	2.2	15
809	The preparation and X-ray structure of Pt(PMe2Ph)2[S2N3(SO2)(NH2)]. Journal of the Chemical Society Chemical Communications, 1989, , 58.	2.0	5
810	New metal–sulphur–nitrogen compounds from reactions in liquid ammonia. The X-ray structures of trans-bis(acetophenone dimethylhydrazone-Nα)dichloropalladium(II) and [di(azathien)-1-yl-S1N4][2-(hydrazonoethyl)phenyl]palladium(II). Journal of the Chemical Society Dalton Transactions, 1989, , 1179-1185.	1.1	15

#	Article	IF	CITATIONS
811	Facile synthesis of SN and S–N–O complexes in liquid ammonia; X-ray structure of Pt[(HN)2SO2](PPh2Me)2. Journal of the Chemical Society Chemical Communications, 1989, , 1060-1061.	2.0	10
812	The reactions of sulphur–nitrogen species in liquid ammonia. Journal of the Chemical Society Chemical Communications, 1988, , 1479-1480.	2.0	13
813	Alkoxy derivatives of trithiazyltrichloride. Polyhedron, 1987, 6, 2161-2164.	2.2	10
814	Chemical Reactions in Applied Magnetic Fields. , 0, , 467-481.		0
815	Thermochromic Coatings for Intelligent Architectural Glazing. Journal of Nano Research, 0, 2, 1-20.	0.8	46
816	Chapter 10. CVD of Functional Coatings on Glass. , 0, , 451-476.		0
817	Determination of the Optical Constants of VO <sub>2</sub> and Nb-Doped VO <sub>2</sub> Thin Films. Materials Science Forum, 0, 587-588, 640-644.	0.3	8
818	Optimisation of Thermochromic Thin Films on Glass; Design of Intelligent Windows. Advances in Science and Technology, 0, , .	0.2	1